NAVAL POSTGRADUATE SCHOOL

MONTEREY, CALIFORNIA

THESIS

ILLUMINATION WAVEFORM DESIGN FOR NON-GAUSSIAN MULTI-HYPOTHESIS TARGET CLASSIFICATION IN COGNITIVE RADAR

by

Ke Nan Wang

June 2012

Thesis Advisor:	Grace A. Clark
Thesis Co-Advisor:	Ric A. Romero

Approved for public release; distribution is unlimited

THIS PAGE INTENTIONALLY LEFT BLANK

REPORT DOCUMENTATION PAGE			Form Approved OMB No. 0704–0188
Public reporting burden for this collection of information is estimated to average 1 hour per response, including the time for reviewing instruction, searching existing data sources, gathering and maintaining the data needed, and completing and reviewing the collection of information. Send comments regarding this burden estimate or any other aspect of this collection of information, including suggestions for reducing this burden, to Washington headquarters Services, Directorate for Information Operations and Reports, 1215 Jefferson Davis Highway, Suite 1204, Arlington, VA 22202–4302, and to the Office of Management and Budget, Paperwork Reduction Project (0704–0188) Washington DC 20503.			
1. AGENCY USE ONLY *(Leave blank)*	**2. REPORT DATE** June 2012	**3. REPORT TYPE AND DATES COVERED** Master's Thesis	
4. TITLE AND SUBTITLE Illumination Waveform Design for Non-Gaussian Multi-Hypothesis Target Classification in Cognitive Radar		**5. FUNDING NUMBERS**	
6. AUTHOR(S) Ke Nan Wang			
7. PERFORMING ORGANIZATION NAME(S) AND ADDRESS(ES) Naval Postgraduate School Monterey, CA 93943–5000		**8. PERFORMING ORGANIZATION REPORT NUMBER**	
9. SPONSORING /MONITORING AGENCY NAME(S) AND ADDRESS(ES) N/A		**10. SPONSORING/MONITORING AGENCY REPORT NUMBER**	
11. SUPPLEMENTARY NOTES The views expressed in this thesis are those of the author and do not reflect the official policy or position of the Department of Defense or the U.S. Government. IRB Protocol number _____N/A_____.			
12a. DISTRIBUTION / AVAILABILITY STATEMENT Approved for public release; distribution is unlimited		**12b. DISTRIBUTION CODE**	

13. ABSTRACT (maximum 200 words)

A cognitive radar (CR) system is one that observes and learns from the environment, then uses a dynamic closed-loop feedback mechanism to adapt the illumination waveform so as to provide system performance improvements over traditional radar systems. A CR system that performs multiple hypothesis target classification and exploits the spectral sparsity of correlated narrowband target responses to achieve significant performance improvements over traditional radars that use wideband illumination pulses was recently developed. This CR system, which was designed for Gaussian target responses, is extended to non-Gaussian targets.

In this thesis, the CR system is generalized to deal effectively with arbitrary non-Gaussian distributed target responses via two key contributions: (1) an important statistical expected value operation that is usually evaluated in closed form is evaluated numerically using an ensemble averaging operation, and (2) a powerful new statistical sampling algorithm and a kernel density estimator are applied to draw complex target samples from target distributions specified by both a desired power spectral density and an arbitrary desired probability density function. Simulations using non-Gaussian targets demonstrate very effective algorithm performance. As expected, this performance gain is realized at the expense of increased computational complexity.

14. SUBJECT TERMS Cognitive Radar, illumination waveform, draw complex target samples, expected value operation, non-Gaussian, dynamic feedback, spectral sparsity, numerical evaluation, target classification			**15. NUMBER OF PAGES** 110
			16. PRICE CODE
17. SECURITY CLASSIFICATION OF REPORT Unclassified	**18. SECURITY CLASSIFICATION OF THIS PAGE** Unclassified	**19. SECURITY CLASSIFICATION OF ABSTRACT** Unclassified	**20. LIMITATION OF ABSTRACT** UU

NSN 7540–01–280–5500 Standard Form 298 (Rev. 2–89)
Prescribed by ANSI Std. 239–18

THIS PAGE INTENTIONALLY LEFT BLANK

Approved for public release; distribution is unlimited

ILLUMINATION WAVEFORM DESIGN FOR NON-GAUSSIAN MULTI-HYPOTHESIS TARGET CLASSIFICATION IN COGNITIVE RADAR

Ke Nan Wang
Ensign, United States Navy
B.S.E.E., United States Naval Academy, 2011

Submitted in partial fulfillment of the
requirements for the degree of

MASTER OF SCIENCE IN ELECTRICAL ENGINEERING

from the

NAVAL POSTGRADUATE SCHOOL
June 2012

Author: Ke Nan Wang

Approved by: Grace A. Clark
Thesis Advisor

Ric A. Romero
Thesis Co-Advisor

R. Clark Robertson
Chair, Department of Electrical and Computer Engineering

THIS PAGE INTENTIONALLY LEFT BLANK

ABSTRACT

A cognitive radar (CR) system is one that observes and learns from the environment, then uses a dynamic closed-loop feedback mechanism to adapt the illumination waveform so as to provide system performance improvements over traditional radar systems. A CR system that performs multiple hypothesis target classification and exploits the spectral sparsity of correlated narrowband target responses to achieve significant performance improvements over traditional radars that use wideband illumination pulses was recently developed. This CR system, which was designed for Gaussian target responses, is extended to non-Gaussian targets.

In this thesis, the CR system is generalized to deal effectively with arbitrary non-Gaussian distributed target responses via two key contributions: (1) an important statistical expected value operation that is usually evaluated in closed form is evaluated numerically using an ensemble averaging operation, and (2) a powerful new statistical sampling algorithm and a kernel density estimator are applied to draw complex target samples from target distributions specified by *both* a desired power spectral density and an arbitrary desired probability density function. Simulations using non-Gaussian targets demonstrate very effective algorithm performance. As expected, this performance gain is realized at the expense of increased computational complexity.

THIS PAGE INTENTIONALLY LEFT BLANK

TABLE OF CONTENTS

LIST OF FIGURES

THIS PAGE INTENTIONALLY LEFT BLANK

LIST OF TABLES

THIS PAGE INTENTIONALLY LEFT BLANK

LIST OF ACRONYMS AND ABBREVIATIONS

AWGN	Additive White Gaussian Noise
CR	Cognitive Radar
CRGC	Cognitive Radar Gaussian Classification (algorithm)
NGCCR	Cognitive Radar Non-Gaussian Classification (algorithm)
ESD	Energy Spectral Density
ESV	Energy Spectral Variance
IID	Independent and Identically Distributed (samples)
KDE	Kernel Density Estimator
MAP	Maximum A Posteriori Probability (estimation)
P_{cc}	Probability of Correct Classification
PDF	Probability Density Function
PSD	Power Spectral Density
PSV	Power Spectral Variance
PWE	Probability Weighted Energy
SNR	Signal-to-Noise Ratio
ZMNL	Zero-Memory Non-Linear

THIS PAGE INTENTIONALLY LEFT BLANK

EXECUTIVE SUMMARY

Cognitive radar (CR) is a concept proposed in 2006 by S. Haykin to improve the performance of radar systems in resource-constrained and interference-limited environments [1]. A CR system is one that has the ability to observe and learn from the environment, then use a dynamic closed-loop feedback mechanism to adapt the illumination waveform so as to provide system performance improvements over traditional radar systems. Traditional radar systems use wideband pulses, or chirps, as illumination waveforms. These have an advantage in that they ensure that all of the modes of the target are excited. The disadvantage is that these wideband illumination waveforms use more energy than necessary when extended target responses are correlated, as they sometimes are in practice. Some extended targets have narrowband frequency spectra; much of the spectrum is sparse. Exciting these low-energy parts of the spectrum is wasteful. This relative spectral sparsity offers opportunity for CR design.

Recent research by R. Romero et al. developed a CR system that exploits the spectral sparsity of correlated narrowband target responses via real-time adaptive illumination waveforms that are matched to the targets [2]–[6]. These matched waveforms strategically place spectral energy in the parts of the spectrum that correspond to the highest energy parts of the target spectra. This approach provides target classification performance advantages for the CR system. For individual targets, the CR algorithms of Romero et al. create illumination waveforms that are optimal in the sense that they maximize the signal-to-noise ratio (SNR) in the radar receiver. In a multiple target hypothesis classification setting, the individually optimal illumination waveforms are linearly combined in a weighted sum to form a single designed illumination waveform referred to as a probability weighted energy (PWE) waveform, where the weights are the prior probabilities of the corresponding classes. Initially, the weights (priors) are assumed equal. An iterative maximum a posteriori probability (MAP) algorithm is used to update the priors and the PWE in each iteration. In practice, after about 5 to 10 iterations, the updated priors converge to values that cause the posterior

probability density of the measurements given the target to be maximized. This leads to a high probability of correct classification (P_{cc}) for the multiple hypothesis classification problem.

The CR system of Romero et al. is very effective. It was derived for the case in which both the target responses and the measurement noise are Gaussian-distributed stochastic processes. For the purposes of this thesis, we dub this system the *Gaussian Classification Cognitive Radar* (GCCR) system. The Gaussian assumption is very appropriate for the measurement noise. However, in some cases, it may not be appropriate for the target response signals. Consequentially, if the target distributions vary from Gaussian, the GCCR system performance may be compromised. This is especially true if the target probability densities are bi-modal or multi-modal. There exist strong theoretical and operational needs in the CR setting for the ability to design adaptive illumination waveforms for non-Gaussian targets.

The purpose of this thesis is to extend the CR multiple hypothesis classification algorithm of Romero et al. to deal effectively with arbitrary non-Gaussian distributed target responses. For Gaussian targets, the Bayesian mathematics of the GCCR MAP algorithm are simplified as closed-form expressions for the posterior density, and other terms can be derived with some effort. For arbitrary non-Gaussian targets, the basic Bayesian mathematics must be extended appropriately for the non-Gaussian case, then implemented numerically using concepts from statistical sampling theory. This is the primary contribution of this thesis. One key result of this research is the recognition that the Bayesian mathematics can be extended to the non-Gaussian case if the integrals that evaluate the expected value operation are replaced by online numerical ensemble average operations. The new algorithm derived in this thesis is dubbed the *Non-Gaussian Classification Cognitive Radar* (NGCCR) system.

Another key contribution of this thesis is the application of a kernel density estimator and a new statistical sampling algorithm by Nichols et al. [7] that draws random samples from a desired stochastic process that is specified by *both* a desired power spectral density (PSD) and a desired arbitrary (non-Gaussian) probability density function (PDF). The sampling algorithm of Nichols et al. is designed for real data, but in

this thesis is extended for complex signals by applying the theory of complex random variables. Fundamental statistical sampling algorithms such as the Metropolis-Hastings algorithm and the Importance Sampling algorithm draw independent identically-distributed (IID) samples from a distribution with an arbitrary PDF. However, for the CR problem, samples from a distribution that is specified by an arbitrary PDF and also *correlated* by the PSD of the narrowband target responses are required. The new algorithm by Nichols et al. provides the capability needed for this work. In addition, the sampling algorithm is relatively simple to implement, making it very valuable.

The new CR multiple hypothesis classification algorithm for non-Gaussian distributed target classes (the NGCCR system) is tested using simulated data sets that are non-Gaussian. It is shown that the P_{cc} for the new algorithm using the MAP designed PWE illumination waveform is significantly greater than that using a broadband pulse waveform over a wide range of values for the illumination waveform energy E_s. As expected, the wideband illumination signal and the PWE give approximately the same P_{cc} when the transmit energy values are high enough. This makes intuitive sense and is consistent with the results for the GCCR system. As the saying goes, "if the input signal energy is large enough, then any waveform is a good waveform." In practical energy ranges, the new NGCCR system provides significant performance improvement over the traditional wideband illumination pulse, making it valuable in a CR setting.

The tradeoff for the new NGCCR system is that it involves significantly more computational complexity than the original GCCR system. The ability to deal effectively with non-Gaussian target responses comes at the price of more computations. This is expected and necessary.

References

[1] S. Haykin, "Cognitive radar" in *IEEE Signal Processing Magazine*, vol. 30, January 2006.

[2] R. Romero and N. A. Goodman, “Information-theoretic matched waveform in signal dependent interference,” in *Proc. of IEEE Radar Conference*, Rome, Italy, May 2008.

[3] R. Romero and N. A. Goodman, “Waveform design in signal-dependent interference and application to target recognition with multiple transmissions,” *IET Radar Sonar Navig.*, vol. 3, no. 4, pp. 328–340, 2009.

[4] R. Romero and N. A. Goodman, “Improved waveform design for target recognition with multiple transmissions,” presented at International WDD Conference, Orlando, Florida, 2009.

[5] R. Romero and N. A. Goodman, “Theory and application of SNR and mutual information matched illumination waveforms,” *IEEE Trans. Aerosp. Electron. Syst.*, vol. 47, no. 2, 2011.

[6] M. R. Bell, “Information theory and radar waveform design,” *IEEE Trans. Inf. Theory*, vol. 39, no. 5, 1993.

[7] J. M. Nichols, C. C. Olson, J. V. Michalowicz, and F. Bucholtz, “A simple algorithm for generating spectrally colored, non-Gaussian signals” in *Probabilistic Engineering Mechanics*, vol. 25, Elsevier, pp. 315–322, 2010.

ACKNOWLEDGMENTS

I would like to thank my family for their support, guidance, and inspiration throughout my life. I would also like to thank my wife. Her understanding and tolerance of many late nights completing this research is a testament to her loving nature.

I would also like to thank my advisor, Dr. Grace A. Clark, for her support and mentorship throughout my graduate research. Her willingness to assist whenever needed and her constant words of encouragement and motivation were vital to the completion of this thesis. I would also like to thank my thesis co-advisor, Dr. Ric A. Romero. He gave me guidance and suggestions that greatly helped me to understand the thesis topic as well as careful and thoughtful feedback that greatly contributed to the quality of this thesis.

THIS PAGE INTENTIONALLY LEFT BLANK

I. INTRODUCTION AND MOTIVATION

A. BACKGROUND

Traditional radar systems use simple pulse train or wideband chirp waveforms as illumination waveforms to obtain target responses. The task of classification of different targets solely relies on the receiver of the radar system. A broadband illumination waveform can cover a broad frequency spectrum to obtain the target frequency responses. However, in an energy constraint environment, if the target set is auto-correlated and the spectra are narrowband, much illumination energy is wasted on the frequency bands where the target spectrum is small or zero. In the cognitive radar setting, the radar transmits signals that are designed to match the characteristics of the targets for improved target recognition results. A cognitive radar system analyzes the statistics of the dominant energies of an ensemble of potential targets in the frequency domain and formulates the illumination waveform that emphasizes those frequencies. This approach can improve the efficiency in a limited energy setting. The system block diagram of a Cognitive Radar (CR) is illustrated in Figure 1 [1].

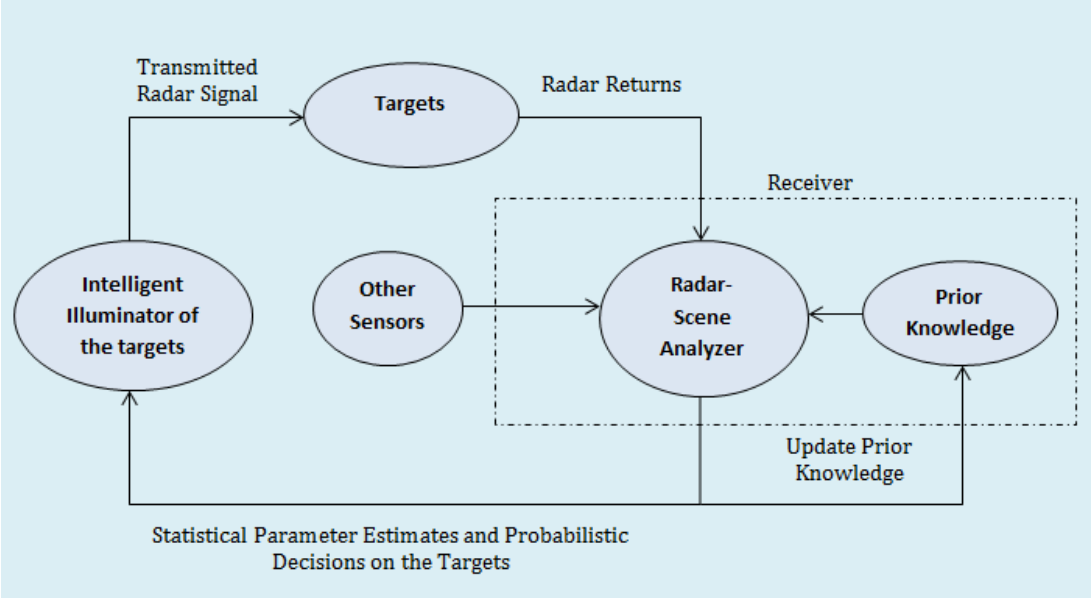

Figure 1. Block diagram of a closed-loop feedback cognitive radar system. After [1].

Based on Figure 1, a cognitive radar system consists of three critical ingredients: (1) intelligent signal processing, which builds on learning through the interaction between the radar and the potential targets; (2) feedback from the receiver to the transmitter, which updates the intelligence; and (3) preservation of the information content of the radar returns [1]. Cognitive radar distinguishes itself from adaptive radar by its ability to learn and adjust to the environment. Feedback must be used carefully in order to ensure stable and reliable operation at all times.

The design of illumination waveforms is critical to the performance of a CR system. The illumination signal must contain enough bandwidth to excite the resonant modes of the target in order to obtain a full characterization of the target. Moreover, it must contain enough power to obtain useful target return signals.

B. OBJECTIVE

The basic approach presented by R. Romero et al. [2]–[6] designs transmit adaptive radar illumination waveforms and updates the prior probabilities of the targets for classification using the assumption that the targets are Gaussian distributed. It also solves a suite of automatic target recognition problems, using both the Signal-to-Noise Ratio (SNR) Maximization Method and the Information-Theoretic Method [5]. This work represents the current state-of-the-art in the area. Here we extend the CR system to classify non-Gaussian distributed targets. This research is focused on finding a general classification algorithm that is suitable for targets with any statistical distributions. This research requires non-Gaussian target simulation, probability density function (PDF) estimation, optimal illumination waveform design algorithms based on SNR maximization, and target classification algorithms, all coded using MATLAB. The research aims to improve the probability of correct classification (P_{cc}) with transmit energy constraints for the non-Gaussian target scenario.

C. RELATED WORK

In the literature, optimal illumination waveform design methods have been investigated for radar systems [2]–[6]. Recent research by R. Romero et al. [2]–[5] created new CR algorithms that exploit the spectral sparsity of correlated narrowband

target responses to design illumination waveforms that are matched to the targets. These designed waveforms strategically place spectral energy in the parts of the spectrum that correspond to the highest energy parts of the target spectra. This approach provides target classification performance advantages for the CR system. For individual targets, matched illumination waveforms are optimal in the sense that they maximize the signal-to-noise ratio (SNR) in the radar receiver [5]. In a multiple target hypothesis classification setting, the individually optimal illumination waveforms are linearly combined in a weighted sum to form a single designed illumination waveform called probability weighted energy (PWE), where the weights are the prior probabilities of the corresponding classes. Initially, the weights (priors) are assumed equal. An iterative maximum a posteriori probability (MAP) algorithm is used to update the priors and the PWE in each iteration. In practice, after about 5 to 10 iterations, the updated priors converge to values that cause the posterior probability density of the measurements given the target to be maximized. This leads to large P_{cc} for the multiple hypothesis classification problem.

The CR system of Romero et al. [2]–[5] is very effective. It was derived for the case in which both the target responses and the measurement noise are Gaussian-distributed stochastic processes. For the purposes of this thesis, we dub this system the *Gaussian Classification Cognitive Radar* (GCCR) system. The Gaussian assumption is very appropriate for the measurement noise. However, at times, it may not be appropriate for the target response signals. Consequentially, if the target distributions vary from Gaussian, the GCCR system performance may be compromised. This is especially true if the target probability densities are bi-modal or multi-modal. There exist strong theoretical and operational needs in the CR setting for the ability to design adaptive illumination waveforms used for non-Gaussian targets.

This thesis work requires the ability to simulate complex target signals given desired target power spectral density (PSD) functions and PDF. Previous work in this area lies in algorithms for Gaussian stochastic processes and algorithms for arbitrarily-distributed (non-Gaussian) stochastic processes. S. Kay [7] presents a method to generate Gaussian distributed complex signals with a given PSD. This technique is used by

Romero et al. in the GCCR system simulations. For the work in this thesis, it is necessary, however, to generate target signals with desired PSDs and desired non-Gaussian PDFs.

A key contribution of this thesis is the application of a new statistical sampling algorithm by Nichols et al. [8] that draws random samples from a desired stochastic process that is specified by *both* a desired PSD and a desired non-Gaussian PDF. The sampling algorithm in [8] is designed for real data, but in this thesis it is extended for complex signals by applying the theory of complex random variables. Fundamental statistical sampling algorithms such as the Metropolis-Hastings algorithm and the Importance Sampling algorithm draw independent, identically distributed (IID) samples from a distribution with an arbitrary PDF [9], [10]. However, for the CR problem, it is required to draw samples from a distribution that is specified by an arbitrary PDF and also from a correlation that is defined by the PSD of the narrowband target responses. The new algorithm by Nichols et al. provides the capability needed for this work. In addition, the sampling algorithm is relatively simple to implement, making it very valuable.

D. APPROACH

The purpose of this thesis is to extend the CR multiple hypothesis classification algorithm of Romero et al. [2]–[5] to deal effectively with arbitrary non-Gaussian distributed target responses. The fundamental classification scheme in [3] and [4] uses a Bayesian MAP scheme that is very general, in the sense that its basic formulation is written in terms of PDFs with arbitrary distributions. However, the GCCR approach of [3] and [4] specializes the Bayesian formulation by assuming Gaussian target distributions. This specialization allows the expected value to be written as an integral in closed form. This integral can then be solved in closed form for the desired posterior density.

For arbitrary non-Gaussian targets, the basic Bayesian equations can be used in their most general form. The integrals that represent the expected value in [3] and [4] cannot, in general, be solved in closed form as they were in the GCCR approach. We

generalize the technique by implementing the expected value as an ensemble average over a simulated ensemble of target realizations. The most difficult and critical problem lies in developing an algorithm for simulating the appropriate target samples that constitute the ensemble. This problem is solved and described in the thesis.

The key contributions of this research lie in using the most general Bayesian MAP formulation, in which the integrals that evaluate the expected value are replaced by online numerical ensemble average operations. The new algorithm derived in this thesis is dubbed the *Non-Gaussian Classification Cognitive Radar* (NGCCR) system.

For this research, all simulations are coded in MATLAB, and all MATLAB m-files and functions used in this research are documented in the Appendix.

E. THESIS OVERVIEW AND ORGANIZATION

The matched waveform design method developed by R. Romero et al. for Gaussian targets (called the GCCR system in this thesis) is described in Chapter II. In this chapter, we introduce the signal and system model for the radar, define the power spectral variance, and summarize the optimal SNR waveform design scheme for a single target.

The multiple hypothesis target classification method used in the GCCR system for Gaussian targets is described in Chapter III. This includes closed form expressions for posterior densities derived using the Gaussian assumption. Then, the GCCR classification theory is extended to deal with non-Gaussian targets.

The motivation and mathematical theory of statistical target signal generation is presented in Chapter IV. First, the concept of complex signal is explained. Next, the algorithm described by Kay [7] for generating a complex Gaussian signal with a specified PSD is presented. Finally, a new algorithm by Nichols et al. is presented. It provides a relatively simple method for generating a real-valued stochastic process with a specified PSD and a specified non-Gaussian PDF. We then show that this algorithm can be extended to work with complex stochastic processes.

The specific implementation issues involved with the new NGCCR system are presented and the experimental setup used to test the new classification algorithm is

described in Chapter V. Specifically, we describe the method of simulating the complex non-Gaussian targets, the implementation of the optimal waveform design algorithm, the MAP multiple hypothesis classification scheme, and the algorithm for updating the prior probabilities of the target classes. Finally, the Monte Carlo simulation scheme for testing the NGCCR system over many parameter variations, target realizations and noise realizations is described.

The results of the experiments described in Chapter V for the NGCCR system are presented in Chapter VI. The PSDs and PDF estimates of the simulated targets and representative illumination waveform are presented. Finally, curves showing the probability of correct classification vs. illumination signal energy for both the optimal waveform and a wideband pulse are presented and compared. This curve demonstrates the performance improvement offered by the new NGCCR system.

Conclusions and a discussion of topics for future research are presented in Chapter VII.

The Appendix contains the MATLAB m-files and functions used in this research.

II. MATCHED WAVEFORM DESIGN

In this chapter, we present a brief summary of the key results developed by Bell, Romero et al. in the area of optimal illumination waveform design for a single target class [2]–[6]. The research in [2]–[6] assumes that both the target distribution and the noise distribution are Gaussian. For this thesis, we assume that the targets can be non-Gaussian or arbitrarily distributed, but the noise is Gaussian.

In [5], optimal illumination waveform design methods were developed using both mutual information and SNR optimality criteria. Both methods are effective. In this thesis, we focus on SNR as the optimality criterion because the theoretical derivations using SNR are more general than the derivations for the mutual information criterion. The solutions for the optimal SNR waveforms in [5] are valid for arbitrary target distributions. However, the derivations using mutual information require the assumption of Gaussian targets [5]. Because our goal is to use arbitrarily-distributed targets, we use the SNR approach.

A. SIGNAL AND SYSTEM MODEL

The theoretical radar target and measurement model is illustrated in Figure 2 [3]. The complex stochastic radar target impulse response $g(t)$ is, at times in practice, a finite-length signal. This $g(t)$ can be modeled as a stochastic process multiplied by a rectangular window of duration T_g [3]. We call the length T_g of the window (in seconds) the mathematical support of $g(t)$. The resulting finite-length impulse response is called a complex stochastic extended target signal $g(t)$. It is called "extended," because it has finite temporal extent. A point target would have zero extent (an impulse). The complex target illumination waveform $x(t)$ with duration T is modeled as the input to the target impulse response. The measured complex radar return signal $y(t)$ is modeled as the convolution of the input with the target impulse response plus additive white Gaussian noise (AWGN) $n(t)$

$$y(t) = x(t) * g(t) + n(t). \tag{1}$$

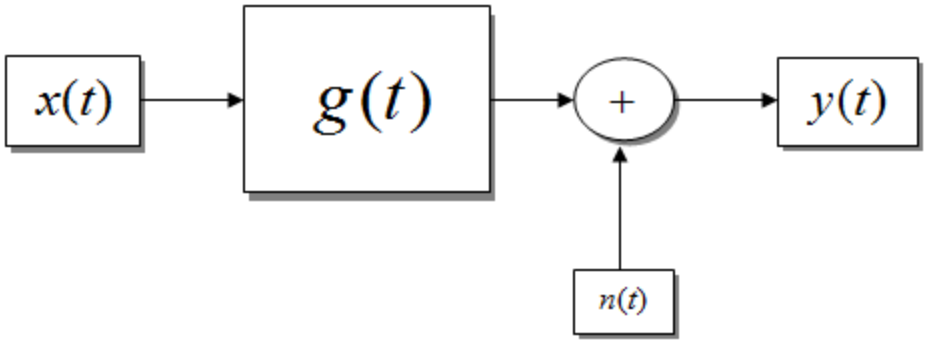

Figure 2. Complex-valued baseband signal and system model with a stochastic target. After [3].

We note that in [2]–[6], the concept of power spectral variance (PSV) rather than PSD is used to describe the spectral content of the target stochastic processes. This is done as a formal way to deal with the fact that we have finite-length extended target signals that cannot strictly be considered to be statistically stationary. When the PSD is used in the literature, it generally is defined over all time for stationary signals. Because we have finite-duration signals, we accommodate them using the concept of PSV. The PSV is defined in terms of the energy spectral density (ESD) given by

$$\xi_G(f) = E\left[\left|G_x(f)\right|^2\right]. \tag{2}$$

Related to this is the energy spectral variance (ESV) defined as

$$\sigma_G^2(f) = E\left[\left|G_x(f) - \mu_{G_x}(f)\right|^2\right] \tag{3}$$

where the spectral mean $\mu_G(f)$ of the target process is defined by

$$\mu_G(f) = E\left[G_x(f)\right]. \tag{4}$$

The key point of this approach is to assume that the finite-duration target processes are stationary within their mathematical support of duration T_g. The PSV of a target signal $g(t)$ is then defined as the average power of the signal over the time duration T_g

$$P_G(f) = \frac{\sigma_G^2(f)}{T_g}. \tag{5}$$

In the remainder of this thesis, the PSV of a signal refers to this definition.

B. OPTIMAL SNR WAVEFORM DESIGN FOR A SINGLE TARGET

Methods for designing the optimal radar illumination waveform for a single stochastic target using the SNR optimality criterion are described in [2]–[6]. The optimal SNR waveform $\hat{x}(t)$ is given as the eigenvector corresponding to the maximum eigenvalue of the eigenfunction [3]

$$\lambda_{\max}\hat{x}(t) = \int_{-T/2}^{T/2} \hat{x}(\tau) R_g(t-\tau) d\tau \tag{6}$$

where the kernel $R_g(t)$ is

$$R_g(t) = \frac{1}{N_0}\int_{-\infty}^{\infty} \sigma_G^2(f) e^{j2\pi ft} df. \tag{7}$$

The PSD of the AWGN is N_0, and T is the duration of the illumination waveform. The optimal illumination waveform for a single target is denoted

$$x^{opt}(t) \square \hat{x}(t). \tag{8}$$

In this chapter, we reviewed the signal and system model for radar and summarized the design method for the optimal SNR illumination waveform for a single target class. In the next chapter, we first describe how this optimal waveform for a single target is used as part of the GCCR multiple hypothesis target classification scheme, which includes a prior probability update that is developed based on the assumption that the targets are Gaussian distributed. We then introduce a new generalized target classification scheme that does not rely on the assumption of Gaussian targets.

THIS PAGE INTENTIONALLY LEFT BLANK

III. MULTIPLE HYPOTHESIS TARGET CLASSIFICATION

In this chapter, we describe the MAP multiple hypothesis [11]–[13] target classification algorithms under consideration in this thesis. First, we describe the method used in the GCCR system, which was designed for target responses that are Gaussian distributed [2]–[5]. Then we describe the new NGCCR system, which relaxes the Gaussian assumption and is shown to be effective for arbitrary target distributions.

We assume that we have available a set of M known representative target responses $\{g_i(t)\}_{i=1}^{M}$ that have been measured or simulated in advance. Also, assume that we calculate in advance the M optimal illumination waveforms $\{x_i^{opt}(t)\}_{i=1}^{M}$ associated with the M target classes. We then use radar measurement signals $y(t) = x(t) * g(t) + n(t)$ in an iterative scheme to produce an illumination waveform that provides high classification performance measured by probability of correct classification (P_{cc}). In this chapter, we describe the iterative classification algorithms for both the Gaussian and non-Gaussian target assumptions.

A. DISCRETE-TIME MEASUREMENT MODEL

The measurement model described earlier is written in terms of continuous time. In real-world applications, we need a discrete time vector formulation which we describe next. For a given target hypothesis H_i, we can write the measurement equation as

$$\underline{y} = X\underline{g}_i + \underline{n} \tag{9}$$

where $\underline{g}_i$ is $L \times 1$, $\underline{y}$ is $L_y \times 1$ and $\underline{n}$ is $L_y \times 1$. The input illumination signal $x(t)$ can be written as an $L \times 1$ input vector $\underline{x}$. This input vector can then be used to construct the circulant $L_y \times L$ circulant convolution matrix X_k:

$$X_k = \begin{bmatrix} x_k(1) & 0 & \cdots & \cdots & 0 \\ x_k(2) & x_k(1) & \ddots & \cdots & 0 \\ \vdots & \vdots & \ddots & \ddots & \vdots \\ x_k(L_x) & x_k(L_x-1) & \cdots & x_k(1) & 0 \\ 0 & x_k(L_x) & x_k(L_x-1) & \cdots & x_k(1) \\ \vdots & 0 & x_k(L_x) & \cdots & x_k(2) \\ \vdots & \vdots & 0 & \ddots & \vdots \\ 0 & 0 & \cdots & 0 & x_k(L_x) \end{bmatrix}. \tag{10}$$

For the classification problem, we use multiple illuminations indexed by k. For this case, we write the measurement for the k^{th} illumination as

$$\underline{y}_k = X_k \underline{g}_i + \underline{n}_k . \tag{11}$$

This measurement model is used in the classification algorithms, as we next show.

B. PWE TRANSMISSION TECHNIQUES

In a multiple target hypothesis classification setting, the individually optimal illumination waveforms $\left\{\underline{g}_i(t)\right\}_{i=1}^{M}$ are linearly combined in a weighted sum to form a single designed illumination waveform called PWE, where the weights are the prior probabilities (or priors) P_i of the M corresponding hypotheses $P_i = P\left(H_i\right)$ [4]. For each iteration, a new illumination waveform is transmitted to illuminate the targets. The priors and the PWE are updated at each iteration k until the priors converge to values that optimize the posterior density that are described later in this chapter. In practice, the algorithm converges to useful results in about 5 to 10 iterations. The desired number of iterations is chosen in advance by the user, so no additional stopping criterion is used. In this scheme, the transmitter tends to place the illumination waveform energy in the spectral bands where the true target most likely resides. This multiple transmission technique is termed the PWE technique [4] and is illustrated in Figure 3.

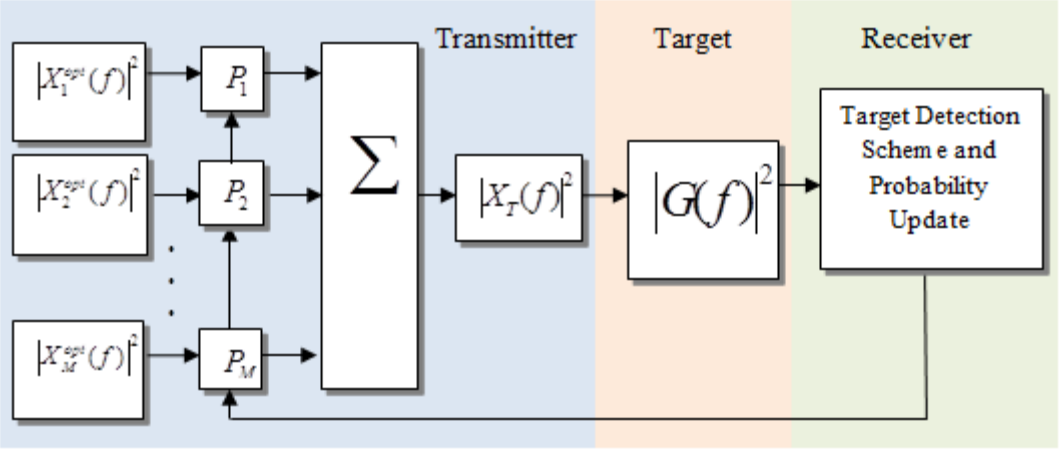

Figure 3. PWE multiple transmission technique for one iteration. From [4].

The PWE multiple transmission technique forms individual optimal waveform spectra $\left|X_i^{opt}(f)\right|^2$, which are developed from the SNR maximization for each target hypothesis. Then each individual waveform is weighted by the prior probability updates P_i^k in order to meet an overall energy constraint E_s. The PWE magnitude spectrum squared is given by

$$PWE^k(f) = E_s \sum_{i=1}^{M} P_i^k \left|X_i^{opt}(f)\right|^2 \tag{12}$$

where P_i^k is the prior probability of the i^{th} target hypothesis for the k^{th} transmission. This PWE illumination waveform is the sum of all individual matched waveforms scaled by their corresponding updated prior probabilities. In the case where the individual matched waveforms are designed in the time domain using an eigenfunction solution (see Eq. (6)) [3], the time domain PWE waveform is

$$PWE^k(t) = \sqrt{E_s} \sum_{i=1}^{M} \sqrt{P_i^k}\, x_i^{opt}(t). \tag{13}$$

Note that the PWE is scaled by a square root. This is done to ensure the scaling factor for the frequency domain has the same scaling effect in the time domain.

Note that the PWE is used as the radar illumination signal to illuminate all of the targets. Mathematically, this is accomplished in the measurement model by writing the PWE signal in Eq. (13) as an $L \times 1$ input PWE vector $\underline{x}$. This input PWE vector is used to construct the circulant convolution matrix X_k as described in Section A.

C. ITERATIVE ALGORITHMS FOR UPDATING THE PRIOR PROBABILITIES

After defining some key quantities and relationships regarding the measurements, we now review the MAP algorithm proposed by Romero et al. [3] for updating the priors P_i under the Gaussian target assumption in the GCCR system. This involves using closed form expressions for the required PDFs and using integrals to evaluate the required expected value operation. Second, we derive an extension of this MAP algorithm under the assumption that the target random variables have arbitrary (non-Gaussian) distributions for the NGCCR system. This involves replacing the integrals in the GCCR system with a numerical ensemble averaging operation to evaluate the required expected values. It also requires a statistical sampling algorithm to draw samples from the desired target distributions specified by both a PDF and a PSD. This sampling algorithm is described in a succeeding chapter.

In the closed-loop radar multiple hypothesis classification scheme, for the i^{th} target for $(k+1)^{th}$ transmission, the normalized prior probability update rule is given by [3]

$$P_i^{k+1} = \frac{p_i^k(y_1, y_2, ..., y_k)P_0}{\sum_{i=1}^{M} p_i^k(y_1, y_2, ..., y_k)P_0} \tag{14}$$

where $p_i^k(y_1, y_2, ..., y_k)$ is the joint PDF of the multiple measurements at the k^{th} illumination. Initially, the weights (priors) are assumed equal because we have no prior information about them. We then let the iterative algorithm adjust the priors appropriately according to the MAP criterion [4], [12], [13]. The initial prior P_0 is given by

$$P_0 = \frac{1}{M} \tag{15}$$

where M is the number of the target hypotheses. Next, we derive the prior probability update algorithms required in the CRGC and NGCCR systems.

1. True Measurements vs. Simulated or Estimated Measurements

Let us first distinguish clearly between *true measurements* and *simulated (or estimated) measurements*. By a true measurement, we mean the measurement that a radar system would acquire in an operational scenario. We denote the model for this by $\underline{y}_k = X_k \underline{g}_i + \underline{n}_k$. This means that the true target is $\underline{g}_i$, and we received a measurement of its response to a radar illumination signal.

Let us now consider the fact that for our problem, we have prior knowledge of representative target responses $\left\{\underline{g}_i(t)\right\}_{i=1}^{M}$ that we have stored in memory. We can later draw samples from their distributions and generate an ensemble of representative signals that we can use in our classification scheme. We can simulate "estimated measurements" $\hat{\underline{y}}_k = X_k \hat{\underline{g}}_i$ that are used as an estimate of the measurement one would expect from the known target classes. Here, we let the "hat" on the target vector $\hat{\underline{g}}_i$ denote the concept of a single *simulated realization* of the complex random target vector $\underline{g}_i$. We show that we can use these estimated measurements in a MAP scheme to update the target priors.

For example, consider that we have four target hypotheses $(M = 4)$, and the third target $\underline{g}_3$ is the true target realization corresponding to our current measurement $\underline{y}_k = X_k \underline{g}_3 + \underline{n}_k$. We can generate four estimated measurements $\left\{\hat{\underline{y}}_{i,k} = X_k \hat{\underline{g}}_i\right\}_{i=1}^{4}$ that can be used for comparison with the radar measurement $\underline{y}_k = X_k \underline{g}_3 + \underline{n}_k$. Next, we show how this comparison is done.

2. The MAP Scheme for Updating the Priors in the GCCR System

The iterative update algorithm for the prior probabilities requires that we illuminate the target multiple times and measure the resulting set of target responses $\{y_1, y_2, ..., y_k\}$, $k = 1, 2, \ldots, K$. The Bayesian MAP approach requires prior knowledge of the prior PDFs $\left\{p_i(\underline{g}_i)\right\}_{i=1}^{M}$, where M is the number or target classes. These priors are available. We also assume that the M target responses are known in advance because we have measured them or modeled them. For the GCCR system, the PDFs have been modeled as zero mean Gaussian with target covariance matrix K_{g_i}, denoted $g_i : N\left[0, K_{g_i}\right]$. For the NGCCR system, we estimate these PDFs as described in a succeeding chapter.

We also require the joint conditional PDF $p_i^k(\underline{y}_1, y_2 ..., \underline{y}_k \mid \underline{g}_i)$ for the k^{th} iteration. This is known as the posterior density of the k measurements $\{y_1, y_2, ..., y_k\}$ conditioned on a particular realization of the i^{th} target $\underline{g}_i$. The proper formation of this posterior PDF is the key to the effectiveness of the MAP algorithm. The k measurements conditioned on the target realization $\underline{g}_i$ are independent, so their joint conditional density can be written as the product of the individual conditional densities $p_i^k\left(\underline{y}_k \left| \underline{g}_i \right.\right)$ as follows:

$$p_i^k\left(\underline{y}_1, \underline{y}_2, \ldots, \underline{y}_k \left| \underline{g}_i \right.\right) = \prod_{k=1}^{K} p_i^k\left(\underline{y}_k \left| \underline{g}_i \right.\right). \tag{16}$$

The key to the GCCR system is the formulation of the individual posterior conditional densities $\left\{p_i^k\left(\underline{y}_k \left| \underline{g}_i \right.\right)\right\}_{i=1}^{M}$ as functions of the true measurements $\left\{\underline{y}_k\right\}_{k=1}^{M}$ and the estimated measurements $\left\{\underline{\hat{y}}_{i,k} = X_k \underline{\hat{g}}_i\right\}_{i=1}^{M}$. Because the measurements are functions of zero mean Gaussian target responses and zero mean noise sequences, Romero et al. consider the posterior conditional densities as Gaussian PDFs and model them as such [3]:

$$p_i^k\left(\underline{y}_k\left|\underline{g}_i\right.\right)=\frac{1}{\pi^L\left|K_N\right|}\exp\left[-\left(\underline{y}_k-X_k\hat{\underline{g}}_i\right)^H K_N^{-1}\left(\underline{y}_k-X_k\hat{\underline{g}}_i\right)\right]. \tag{17}$$

In this expression, the estimated measurement $\left\{\hat{\underline{y}}_{i,k}=X_k\hat{\underline{g}}_i\right\}_{i=1}^M$ takes on the role of the mean of the Gaussian random variable $\underline{y}_k$, and the covariance matrix K_N takes on the role of the covariance K_y. We can denote this as follows: $\underline{y}_k\left|\underline{g}_i\right. \square\ N\left[X_k\underline{g}_i,K_N\right]$. Note that $K_N=\sqrt{P_n/2}\cdot I$ where P_n is the noise power, and I is an identity matrix of size $L_y\times L_y$. This formulation is intuitively appealing, because the difference $\underline{y}_k-X_k\hat{\underline{g}}_i$ can be interpreted as an error term between the true measurement and the estimated measurement. For convenience, call this error term $\underline{e}_{i,k}=\underline{y}_k-X_k\hat{\underline{g}}_i$. Because the measurement model is $\underline{y}_k=X_k\underline{g}_i+\underline{n}_k$, if $\underline{g}_i$ happens to be the true target in the operational scenario, then the error is approximately the noise, which is Gaussian distributed $\underline{n}$: $N\left[0,K_N\right]$. The posterior PDF described by Eq. (17) models this noise very nicely. If $\underline{g}_i$ happens to be one of the estimated targets (not the true target) in the operational scenario, then we expect the error to be somewhat larger than it is when $\underline{g}_i$ is the true target. However, the error can be thought of as approximately the noise with some perturbation. This is intuitively appealing, because it means that the differences among the various targets manifest as varying values of the posterior densities. In addition, Romero et al. demonstrated that this formulation made the GCCR system very effective for multiple hypothesis target classification [3]–[5].

Continuing with the GCCR system development, we can write the posterior conditional PDF for the set of k independent measurements as [3]

$$\begin{aligned}p_i^k\left(\underline{y}_1,\underline{y}_2,\ldots,\underline{y}_k\left|\underline{g}_i\right.\right)&=\prod_{k=1}^K p_i^k\left(\underline{y}_k\left|\underline{g}_i\right.\right)\\&=\frac{1}{\pi^{LK}\left|K_N\right|^K}\exp\left[-\sum_{k=1}^K\left(\underline{y}_k-X_k\hat{\underline{g}}_i\right)^H K_N^{-1}\left(\underline{y}_k-X_k\hat{\underline{g}}_i\right)\right].\end{aligned} \tag{18}$$

Given the quantities described above, the joint density of the multiple measurements can be written as the expected value of the joint density of the multiple measurements conditioned on the target:

$$p_i^k\left(\underline{y}_1, \underline{y}_2, \ \ldots, \underline{y}_k\right) = E_{\underline{g}}\left\{ p_i^k\left(\underline{y}_1, \underline{y}_2, \ldots, \underline{y}_k \,\middle|\, \underline{g}_i\right)\right\}. \tag{19}$$

For the Gaussian target assumption, we can write the expected value operation in integral form:

$$p_i^k\left(\underline{y}_1, \underline{y}_2, \ \ldots, \underline{y}_k\right) = \int_{\underline{g}_i} p_i^k\left(\underline{y}_1, \underline{y}_2, \ldots, \underline{y}_k \,\middle|\, \underline{g}_i\right) p(\underline{g}_i) d\underline{g}_i \,. \tag{20}$$

Since the target signal is based on a Gaussian assumption, the prior density of the target $p(\underline{g}_i)$ is assumed to be a zero-mean complex Gaussian signal, and its PDF is given by

$$p(\underline{g}_i) = \frac{1}{\pi^L \left| K_{\underline{g}_i} \right|} \exp\left[-\underline{g}_i^H K_{\underline{g}_i}^{-1} \underline{g}_i \right]. \tag{21}$$

The final expression for the joint PDF is derived in closed form by evaluating the expected value in integral form as written in Eq. (20) and can be simplified to [3]

$$\begin{aligned} p_i^k(\underline{y}_1, \ldots, \underline{y}_k) &= E_{\underline{g}_i}\left[p_i^k(\underline{y}_1, \ldots, \underline{y}_k \mid \underline{g}_i) \right] \\ &= \frac{\left| Q^{-1} \right|}{\left| K_{g_i} \right| \pi^{LK} \left| K_N \right|^K} \exp\left[-\sum_{k=1}^{K} \underline{y}_k^H K_N^{-1} \underline{y}_k \right] \\ &\quad \times \exp\left[\left(\sum_{k=1}^{K} X_k^H K_N^{-1} \underline{y}_k \right)^H Q^{-1} \sum_{k=1}^{K} X_k^H K_N^{-1} \underline{y}_k \right] \end{aligned} \tag{22}$$

where K_{g_i} is the target covariance matrix of target hypothesis vector, E_g denotes the expected value over the variable g, and Q is defined by

$$Q = K_{g_i}^{-1} + \sum_{k=1}^{K} X_k^H K_N^{-1} X_k \,. \tag{23}$$

The expression in Eq. (22) is used in the prior probability update algorithm of Eq. (14). Once the priors are updated, they are used to update the PWE in Eq. (13). This PWE is then used by the radar as the new illumination signal for the next iteration.

3. Classification Algorithm for the NGCCR System

In this section, we derive an extension of the MAP algorithm under the assumption that the target random variables have arbitrary (non-Gaussian) distributions for the NGCCR system. This involves replacing the integrals in the GCCR classification algorithm with a numerical ensemble averaging operation to evaluate the required expected values.

The fundamental Bayesian MAP approach for the NGCCR system is the same as that for the GCCR system. We desire to evaluate the joint density of the multiple measurements, which can be written as the expected value of the joint density of the multiple measurements conditioned on the target:

$$p_i^k\left(\underline{y}_1, \underline{y}_2, \ \ldots, \underline{y}_k\right) = E_g\left\{p_i^k\left(\underline{y}_1, \underline{y}_2, \ldots, \underline{y}_k \left| \underline{g}_i\right.\right)\right\}. \tag{24}$$

Recall that for the GCCR system, this can be written in closed form using the expected value operation in integral form:

$$p_i^k\left(\underline{y}_1, \underline{y}_2, \ \ldots, \underline{y}_k\right) = \int_{\underline{g}_i} p_i^k\left(\underline{y}_1, \underline{y}_2, \ldots, \underline{y}_k \left| \underline{g}_i\right.\right) p(\underline{g}_i) d\underline{g}_i. \tag{25}$$

However, for the NGCCR system, we assume that the target responses have arbitrary (non-Gaussian) distributions, so the desired PDFs cannot be written in closed form. As a result, we cannot use the integral form of the expected value $E_{g_i}\{\bullet\}$. Nonetheless, the posterior joint conditional density of the multiple measurements given a realization of a target is similarly given by [3]

$$
\begin{aligned}
p_i^k\left(\underline{y}_1,\underline{y}_2,\ldots,\underline{y}_k\,\middle|\,\underline{g}_i\right) &= \prod_{k=1}^{K} p_i^k\left(\underline{y}_k\,\middle|\,\underline{g}_i\right) \\
&= \frac{1}{\pi^{LK}\left|K_N\right|^K}\exp\left[-\sum_{k=1}^{K}\left(\underline{y}_k - X_k\hat{\underline{g}}_i\right)^H K_N^{-1}\left(\underline{y}_k - X_k\hat{\underline{g}}_i\right)\right].
\end{aligned}
\tag{26}
$$

This expression remains general and can be used in the NGCCR system because the targets appear as the variable on which the measurements are conditioned and the prior densities of the targets $p(\underline{g}_i)$ do not appear explicitly. The $\left\{p(\underline{g}_i)\right\}_{i=1}^{M}$ do, however, come into play in the required statistical sampling of their distributions as part of a general complex random number generator described in a succeeding chapter. The multiple measurements are conditioned on single realizations of the target vectors $\underline{g}_i$, which are treated as deterministic vectors.

The key to the effectiveness of the NGCCR system lies in the numerical evaluation of the expected value operation $E_{g_i}\{\bullet\}$ in Eq. (24); i.e., using the ensemble average of an ensemble of many realizations of the posterior joint conditional joint density defined by Eq. (26). The approach is to create N_g realizations of the target $\underline{g}_i$ and use these to form an ensemble $\left\{p_{i,j}^k\left(\underline{y}_1,\underline{y}_2,\ldots,\underline{y}_k\,\middle|\,\underline{g}_i\right)\right\}_{j=1}^{N_g}$ of realizations of the joint conditional posterior density. We can then compute a numerical estimate of the expected value $E_{g_i}\{\bullet\}$ by computing the ensemble average of the values of the posterior densities such that

$$
\begin{aligned}
p_i^k\left(\underline{y}_1,\underline{y}_2,\ \ldots,\underline{y}_k\right) &= E_g\left\{p_i^k\left(\underline{y}_1,\underline{y}_2,\ldots,\underline{y}_k\,\middle|\,\underline{g}_i\right)\right\} \\
&\approx \frac{1}{N_g}\sum_{j=1}^{N_g} p_{i,j}^k\left(\underline{y}_1,\underline{y}_2,\ldots,\underline{y}_k\,\middle|\,\underline{g}_i\right).
\end{aligned}
\tag{27}
$$

Once we have these joint densities, we use them to update the prior probabilities. We use the updated priors to update the PWE illumination signal, which is then transmitted by

the radar to illuminate the targets. The user defines in advance the desired number of iterations to use. When that number of iterations is complete, the final target classification decision is made.

Numerically, of course, this evaluation of the expected value comes with tradeoffs. It allows us to deal effectively with non-Gaussian distributed target classes. This procedure comes at the price of increased computational complexity and depends on the number of target realizations generated for use in the target ensemble above. The purpose of this thesis is to show the derivation of the classification scheme for the NGCCR system. Future research should focus reducing the computational complexity and/or speed of implementation of the NGCCR system.

In this chapter, we discussed the Gaussian based target classification scheme used in previous researches and introduced a classification method that eliminates the Gaussian assumption. This method expands the application of the target classification scheme for complex targets with any arbitrary density distributions. In the next chapter, the specific implementation of the experiment is outlined. This includes the discussion of the target generation, optimal waveform design, and target classification processes used in this research.

THIS PAGE INTENTIONALLY LEFT BLANK

IV. TARGET SIMULATION

In this chapter, we introduce the concept of creating stochastic complex signals. First, the feasibility of generating meaningful complex signals is discussed. Next, we explain the theory of generating Gaussian complex signals with a specified PSD. Finally, the method of generating non-Gaussian complex signals with a specified PSD that is used in this research is explained.

A. GENERATION OF STOCHASTIC COMPLEX SIGNALS

1. Motivation for Using a Complex Data Model

In radar, sonar, and many communication systems, complex signals are used extensively to represent the in-phase and quadrature components of the demodulated data. The complex envelope represents the concatenation of the in-phase and quadrature components into the form of real and imaginary quantities. Using the complex data model simplifies analysis. This method is similar to the simplification of using a Fourier series of complex exponentials to represent sines and cosines.

2. Concept of Complex Density

The goal for the complex density is to express the PDF, CDF, and all related statistical measures as a function of the complex variables [7]. The known results for real random variables and those obtained from complex random variables must match. Let the variable $\hat{x}$ be a $2N \times 1$ vector of real and imaginary components as two individual random variables defined as

$$\hat{x} = [x_R, x_I]^T \tag{28}$$

and let the variable $\tilde{x}$ be a single complex random variable defined as

$$\tilde{x} = x_R + jx_I \,. \tag{29}$$

If the covariance matrix $K_{\hat{x}}$ of the original real $2N \times 1$ vector is constrained such that

$$K_{x_R} = K_{x_I} = K_R / 2 \tag{30}$$

and

$$K_{IR} = -K_{RI}^T = K_I / 2, \tag{31}$$

then the duality of the density functions for the real random variables and the complex random variables can be written as

$$f_{\hat{x}}(u,v) = f_{\tilde{x}}(u + jv). \tag{32}$$

The first moment, or the mean vector, can be expressed as

$$E\{\tilde{x}\} = E\{x_R\} + jE\{x_I\} = m_{\tilde{x}}. \tag{33}$$

The second moment, or the correlation matrix, can be expressed as

$$E\{\tilde{x}\tilde{x}^H\} = R_{\tilde{x}} = R_{x_R} + R_{x_I} + j(R_{IR} - R_{RI}). \tag{34}$$

Based on this concept, the complex signals that are used in this research can be analyzed separately by splitting the signal vector into its real and imaginary components [7].

B. GENERATION OF COMPLEX SIGNALS WITH SPECIFIED SPECTRA AND PDF

1. Generation of a Complex Gaussian Signal with a Specified PSD

In previous research, the target classification scheme for the cognitive radar system was focused on detecting complex Gaussian distributed signals with certain power spectral densities. A traditional method used to generate this type of signal was developed by Steven Kay [7]. This algorithm is based on the concept that for a Gaussian random process, the PSD is specified by the covariance matrix **R**. Since this covariance matrix is a symmetric Toeplitz matrix, the eigenvalues λ_i and the eigenvectors ν_i can be

easily found. Let $S_{xx}(f)$ be the PSD of $x[n]$; then as $N \to \infty$, the eigenvalues λ_i and the eigenvectors ν_i are

$$\begin{cases} \lambda_i = S_{xx}(f_i) \\ \nu_i = \frac{1}{N}[1 \ \exp(j2\pi f_i) \ \exp(j4\pi f_i) \ \ldots \ \exp(j2\pi(N-1) f_i)]^T \end{cases} \tag{35}$$

for $i = 0,1,...,N-1$ and $f_i = i/N$. Then covariance matrix **R** is defined as

$$\mathrm{R} = \sum_{i=0}^{N-1} \lambda_i \nu_i \nu_i^H \ . \tag{36}$$

If the data set $\{x[0], x[1], ..., x[N-1]\}$ is randomly generated based on a Gaussian distribution where $x[n]: \mathrm{N}(0, \sigma^2)$, then the zero-mean complex Gaussian discrete target signal $g[n]$ with a specified covariance matrix **R** (or PSD) can be created by

$$g[n] = \sqrt{\mathrm{R}} \cdot x[n] \tag{37}$$

for $n = 0,1,...,N-1$.

Using this method, we can generate a complex Gaussian distributed sequence with a specified PSD to simulate the target signals for the existing target detection scheme. As useful as this method is for simulating complex Gaussian targets, it cannot be used to generate the non-Gaussian complex target signals that are needed for this research. Therefore, a technique for generating complex signals with both specified arbitrary PDF and PSD is required.

2. Generate a Complex Signal with a Specified PDF and PSD

Sampling methods such as the Importance Sampling, Metropolis-Hasting Sampling, and the Slice Sampling create uncorrelated, independent and identically distributed (IID) samples. For the purpose of this research, a correlated non-Gaussian distributed target is desired to evaluate the classification system. The traditional "Kay" method of generating Gaussian stochastic signals with specified PSDs discussed in the previous section cannot be used to generate non-Gaussian distributed signals. Much

research has been done to solve the problem of how to generate observations $x(n), n = 0...N-1$ with a given PDF and auto-covariance (or PSD). Although the details vary in different methods, all approaches tend to follow a similar prescription [8], [14]–[17]. One algorithm developed by Nichols et al. for generating spectrally colored, non-Gaussian complex signals is chosen to use for the classification system [8]. However, it must be noted here that the PDF $p(x)$ and the PSD $S_{xx}(f)$ cannot be specified independently because these two properties are linked through the mean $\overline{x}$ and the variance σ_x^2 of the signal.

A block diagram that generally summarizes the procedure of generating signals with both a desired PDF and a PSD is illustrated in Figure 4 [8]. First, a spectrally white, Gaussian distributed sequence is linearly filtered by the specified auto-covariance (equivalently PSD) to obtain a sequence with a Gaussian PDF and the specified PSD. This step makes use of the fact that if a Gaussian sequence is filtered by a linear system, the output is a Gaussian sequence as well. The data are then subject to a zero-memory, nonlinear (ZMNL) transformation in order to produce a signal with the desired non-Gaussian PDF.

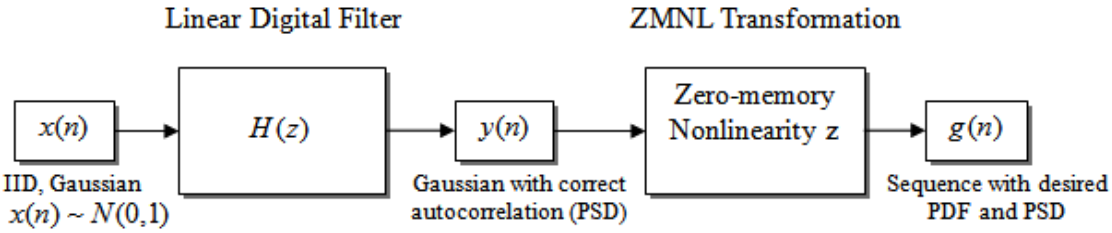

Figure 4. General process for generating signals with a user defined PDF and PSD. From [8].

The goal of the algorithm is to produce a sequence of observations $x[n]$ $n = 0,...,N-1$ with PDF $p(x)$ and a PSD $S_{xx}(f)$. First, a desired PSD function $S_{xx}(f_k)$ is proposed with N discrete frequencies at the bandwidth $f_k = (k - N/2)\Delta_f$, where

$k = 0,...,N-1$. The frequency bin Δ_f is dictated by the temporal sampling interval Δ_t such that $\Delta_f = 1/(N\Delta_t)$. In general, Δ_t should be chosen in accordance with the Nyquist criterion for the maximum resolvable frequency. For the purpose of this research, the frequency domain is normalized to 1 Hz for the analysis of all signal spectra. Thus, the frequency bin is $\Delta_f = 1/N$, and the temporal sampling interval is $\Delta_t = 1$. The discrete Fourier transform and the inverse Fourier transform are defined as

$$X[k] = FT(x[n]) \equiv \sum_{n=0}^{N-1} x[n] e^{-2j\pi kn/N} \tag{38}$$

and

$$x[n] = FT^{-1}(X[k]) \equiv \frac{1}{N} \sum_{k=0}^{N-1} X[k] e^{j2\pi kn/N} . \tag{39}$$

At this point, the relationship between the signal $x[n]$ and its PSD $S_{xx}(f)$ in terms of mean and variance is defined by [8]

$$\overline{x} = \frac{\sqrt{S_{xx}(0)}}{N\Delta t} \tag{40}$$

and

$$\sigma_x^2 = \frac{N}{N-1} \sum_{k=0}^{N-1} S_{xx}(f_k)\Delta f . \tag{41}$$

A data sequence $s[n]$ is generated from a desired distribution $p(x)$. It is natural to have the proposed PDF $p(x)$ to specify the mean of the signal and to have the proposed PSD $S_{xx}(f)$ to specify the variance of the signal. Then the variance of the signal $s[n]$ must be adjusted to conform to the variance of the proposed PSD $S_{xx}(f)$. The variance of the signal is $\sigma_s^2 = \frac{1}{N-1}\sum_n (s[n] - \overline{s})^2$. With the variance of the PSD obtained from Eq. (41), the signal $s[n]$ can be adjusted to a scaled sequence $x_0[n]$ that conforms to the variance of $S_{xx}(f)$ using

$$x_0[n] = \frac{\sqrt{\sigma_s^2}}{\sqrt{\sigma_x^2}} s[n]. \tag{42}$$

The final output signal needs to have the mean specified by the original proposed PDF. At this point, the mean of the sequence $x_0[n]$ is removed for that purpose. In the last step of the procedure, the mean is put back into the signal. The final step for the initialization process is to rearrange the values in $x_0[I_n],\ n = 0,...,N-1$ from smallest to largest and to obtain the indexing I_n for the sequence $x_0[n]$ so that $x_0[I_0] < x_0[I_1] < ... < x_0[I_{N-1}]$.

After the initialization process, the sequence $x_0[n]$ is generated with the target PDF $p(x)$ and the variance of the target PSD $S_{xx}(f)$. The next step is to generate a new signal $x[n]$ that captures the phases of the time-series $x_0[n]$ and the Fourier amplitudes $X_t[k]$ of the proposed PSD. The Fourier amplitudes of the PSD $S_{xx}(f)$ are given by

$$X_t[k] = \sqrt{S_{xx}(f_k)/\Delta_t},\ k = 0,...,N-1, \tag{43}$$

and the phases of the values in the time-series $x_0[n]$ are given by

$$\phi[k] = \tan^{-1}\left(\frac{\mathrm{Im}(X_0[k])}{\mathrm{Re}(X_0[k])}\right). \tag{44}$$

A new signal $x[n]$ is created with the phases of $x_0[n]$ and the Fourier amplitudes of the proposed PSD from

$$x[n] = \frac{1}{N}\sum_{k=0}^{N-1} e^{i\phi[k]} X_t[k] e^{i2\pi kn/N} = FT^{-1}(e^{i\phi[k]} X_t[k]). \tag{45}$$

This signal has the same PSD as the proposed $S_{xx}(f)$. However, due to the central limit theorem [11], the process of the inverse Fourier transform has the effect of whitening the signal towards a Gaussian distribution.

At this point in the process, the signal $x[n]$ is approximately Gaussian distributed and has the desired narrowband PSD. The signal $x_0[n]$ has the target PDF and a constant

PSD (indicating that it is uncorrelated or white). The next step is to apply a nonlinear transformation that has the effect of auto-correlating the signal $x_0[n]$ and ensuring that it has approximately the desired target PSD without altering its PDF. The nonlinear transformation involves sorting (or rank reordering) the values in $x_0[n]$, and this reordering process causes the reordered sequence to be correlated. Specifically, the smallest value in $x_0[n]$ gets assigned the same position of the smallest value in $x[n]$, and the second smallest value in $x_0[n]$ gets assigned the same position of the second smallest value in $x[n]$ etc. The sorted values of $x[n]$, from smallest to largest, are denoted $x[J_n]$, where $x[J_0] < x[J_1] < ... < x[J_{N-1}]$. Then the signal

$$x[J_n] = x_0[I_n],\ n = 0,..., N-1 \tag{46}$$

by definition has the desired target PDF and approximately the desired PSD. This reordering procedure attempts to simulate the effect of the ZMNL transformation, which is a process of mapping a signal with samples drawn from the target PDF into another signal that possesses the target PSD.

Nichols et al. developed this method with the intention of creating real signals with both the target PDF and PSD. However, the simulated radar target signals that are used in this research must be complex signals. Based on the concept discussed in the first section of this chapter, a non-Gaussian and colored spectrum complex signal is created by combining a real signal and an imaginary signal such that both are generated individually from the same non-Gaussian PDF and the same proposed PSD. With the combination of these two concepts, a non-Gaussian, colored spectral complex signal is generated to simulate the target signals in this research.

For the work done in this thesis, the desired specified PSVs are symmetric in the frequency domain. This was done because of a limitation of the statistical sampling algorithm of Nichols et al. The algorithm produces only real sequences, but for our work, we require complex sequences. As described above, we form a complex sequence from two real sequences generated using the Nichols algorithm. The PSVs of these sequences

are always symmetric. However, for some operational scenarios, we need to deal with asymmetric PSVs.

Some preliminary work was done to create asymmetric PSVs by scaling the PSV peaks. This was effective, but it introduced another problem. Once the scaled PSV is created, the only way to use it to create a time-domain waveform is by applying an inverse Fourier transform (IFT) to the PSV. This provides a time-domain waveform, but it is not rigorous because one cannot theoretically compute the IFT of a PSV. The PSV contains only the modulus of the complex frequency domain quantity with no phase information. This means that the IFT is not rigorously defined. Future work should focus on creating a generalized method for sampling a distribution specified by both a desired asymmetric PSV and a desired PDF. This will likely involve using a phase retrieval algorithm for evaluating the IFT of a PSV. A very effective phase retrieval algorithm is described in [18].

The concept of generating complex signals needed to simulate the potential target signals for this research was explained in this chapter. Two specific methods developed by Kay and Nichols respectively were examined. This research uses the latter method to generate complex non-Gaussian and colored spectral signals for the classification system. In the next chapter, the adaptive waveform design method used in this research is thoroughly explained.

V. EXPERIMENTAL SETUP

Experiments and tests conducted in this research require the generation of non-Gaussian colored spectral complex target signals, optimal waveform computation based on proposed target PSVs, coding of the new joint posterior PDF estimate algorithm, and last but not least, a Monte Carlo simulation system for test evaluations. All simulations are conducted in MATLAB and are explained in this chapter.

A. TARGET SIMULATION

The first step for the experiment is to use the solution in [8] to define a number of target hypotheses that are characterized by their PSVs as experimental subjects. For this research, the number of target hypotheses in each classification test set is set to four. All proposed PSVs for the experiment are given by the mixed-Gaussian probability density function

$$S_{xx}(f) = \frac{P_{signal}}{2\sqrt{2\pi\sigma}}\left(e^{-\frac{(f-\mu)^2}{2\sigma^2}} + e^{-\frac{(f+\mu)^2}{2\sigma^2}} \right) \tag{47}$$

where P_{signal} defines the total power in the illumination waveform, μ defines the band-pass frequencies of the two-sided spectral density on a normalized frequency scale, and σ defines both the bandwidth and the amplitudes of the energy bands. It must be noted here that the bandwidths and the amplitudes of the energy bands in each PSV are related because the overall power constraint for the PSV is set by P_{signal}. Thus, changing the parameter σ either increases the amplitude and narrows the energy bands or decreases the amplitude and expands the energy bands. Throughout the experiment, the target-to-noise ratio (TNR) is set to 10 dB. The noise in the receiver is set to unity variance with a power of 1 unit. Thus, P_{signal} is set to 10 units to ensure a TNR of 10 dB. The parameters μ and σ are the two tuning variables for creating different PSVs. An example of a proposed PSV is illustrated in Figure 5. In this particular example, the PSV is defined by $N = 1024$ data samples and the two parameters $\mu = 0.2$ and $\sigma = 0.03$.

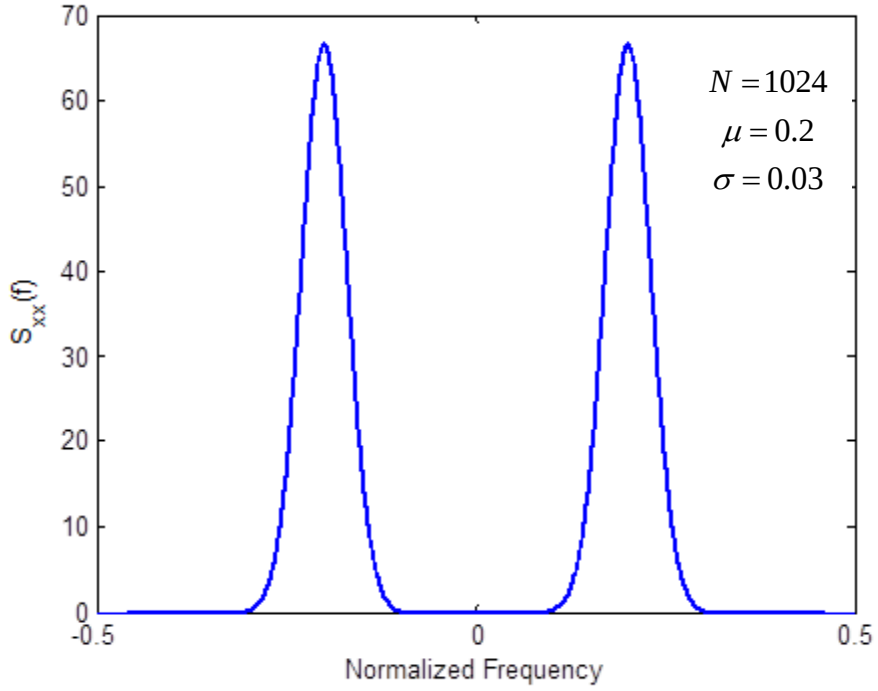

Figure 5. An example of a PSV defined by a mixed Gaussian distribution

Using a PSV such as the one illustrated in Figure 5 along with the MATLAB random number generator based on a chosen density distribution, we used the algorithm created by Nichols et al. described in Chapter IV to generate real data samples from the proposed distribution with a PSV that is very similar to the proposed PSV. In the case for generating one complex target signal, the target generator combines one set of data samples generated for the real component with another set of data samples generated for the imaginary component. Taking into consideration computational speed, we set the number of samples used through the experiment to $N = 64$. The last step for target generation is to scale the data samples properly to ensure that the signal conforms to the signal power defined by P_{signal}. Since complex signals split the energy between the real part and the imaginary part and the scale factor in the frequency domain is the square root of the scale factor in the time domain, the proper scaling for complex signals is given by

$$g_{scaled}(t) = \frac{g(t)}{\sqrt{2N}}. \tag{48}$$

B. SNR MATCHED WAVEFORMS DESIGN

As soon as the four different target PSVs are defined, the optimal individual waveforms for each of the four particular target hypotheses can be generated. The matched waveform design algorithm was explained in Chapter II. To implement this SNR maximization algorithm, first the covariance matrix **R** of each PSV $S_{xx}(f_i)$ must be computed. For AWGN, the expression is given by Eq. (7). An alternative way to compute the integral is by taking the complex eigen decomposition

$$\mathbf{R} = \sum_{i=0}^{N-1} S_{xx}(f_i) v_i v_i^H , \tag{49}$$

where the eigenvector v_i is given by

$$v_i = \exp(j2\pi(i) f_i)^T \tag{50}$$

for $i = 0,...,N-1$ and $f_i = \frac{i}{N}$. Here, f_i is normalized from 0 Hz to 1 Hz.

The matched waveform for a particular target hypothesis based on its PSV $S_{xx}(f)$ is just the eigenvector that corresponds to the maximum eigenvalue, which is the maximum value in the PSV $S_{xx}(f)$. Here, it is important to clarify that the resulting optimal waveform generated from this design algorithm is a temporal waveform because in the next step, the probability update rule is different for waveforms that are in different domains.

Last but not least, the total illumination waveform is created by summing all individual optimal waveforms that are derived from each of the four particular target hypothesis. The illumination waveform is updated by a probability update rule for each transmission. However, for the initial transmission, the illumination waveform weighs each target hypothesis equally. The illumination waveform is given by

$$PWE_{initial}(t) = \sqrt{P_0} \sum_{i=1}^{4} x_i^{opt}(t) \tag{51}$$

where $P_0 = ¼$ defined by Eq. (15).

C. TARGET CLASSIFICATION SCHEME

After the illumination waveform is generated (along with a target realization $\underline{g}$ from an unknown target hypothesis), the next step is to simulate the measurement signal at the radar receiver by

$$\underline{y}_{measured} = X\underline{g}_i + \underline{n}, \tag{52}$$

where $n(t)$ is the complex white noise in the receiver.

The goal for the experiment is to test the new classification scheme. This classification algorithm is an estimate of the MAP detection scheme, the details of which were explained in Chapter III. To implement this algorithm, simulated target responses from each target hypothesis are needed and are given by

$$\underline{\hat{y}}_i = X\underline{g}_i \tag{53}$$

for $i = 1,...,4$ and $\underline{g}_i$ is a target realization based on one particular target hypothesis. Then each one of the four joint PDFs of the measurement $\underline{y}$ for each target is estimated by Eq. (27). The covariance matrix K_N of the noise is given by

$$K_N = \sqrt{\frac{P_n}{2}} \cdot I \tag{54}$$

where I is an identity matrix of size $L_y \times L_y$. Because the MAP detection scheme makes the decision based on the relative probabilities computed from the conditional PDFs, all constants in the expression that are shared by the four joint PDF computations can be disregarded. Thus, for the k^{th} transmission and i^{th} hypothesis, the expression in Eq. (27) can be simplified to

$$p_i^k(y_1,...,y_k) = \frac{1}{J}\sum_{j=1}^{J} \exp\left[-\sum_{k=1}^{K} (\underline{y}_k - \underline{\hat{y}}_i^j)^H K_N^{-1} (\underline{y}_k - \underline{\hat{y}}_i^j) \right], \qquad (55)$$

where J is a user defined number that specifies the number of realizations in the target ensemble and $\underline{\hat{y}}_i^j$ is the simulated target response based on the j^{th} realization of the i^{th} target hypothesis $g_i(t)$. This is numerical implementation of the expected value using ensemble averaging. It must be noted here that the parameter J dictates the accuracy of the expected value estimate, which means that a higher value of J yields a more accurate estimate of $p_i^k(y_1,...,y_k \mid g_i)$. However, increasing J also increases the computational time for each transmission, which is undesirable for target detection in a real world scenario. For this experiment, the value J is chosen as 40 to balance the tradeoffs between accuracy and speed; J was found empirically.

The last step for the target classification scheme is to update the prior probability for each target hypothesis. The update rule is given by Eq. (14). With the new prior probability weights computed for each target hypothesis, the matched waveform for the next transmission is also updated by Eq. (13). At this point, one radar transmission loop is completed. The pseudo-code block diagram of one radar classification evolution is illustrated in Figure 6. This includes the transmission of the first matched waveform, receiver data simulation, target classification, and the probability update for the next transmission. The radar simulator performs a user specified number of transmissions and makes a final decision for target classification based on the last computed prior $\left\{P_i^k\right\}_{i=1}^{M}$. The target classification decisions are then used to compare with the true hypothesis in order to evaluate the performance of the radar system. This concludes one cycle, termed "noise realization," for the target classification experiment.

D. MONTE CARLO SIMULATION SYSTEM SETUP

Because this research deals with stochastic targets, the performance of the classification system cannot be truly evaluated from one target realization. A Monte Carlo simulation is set up for the purpose of testing the performance of the classification

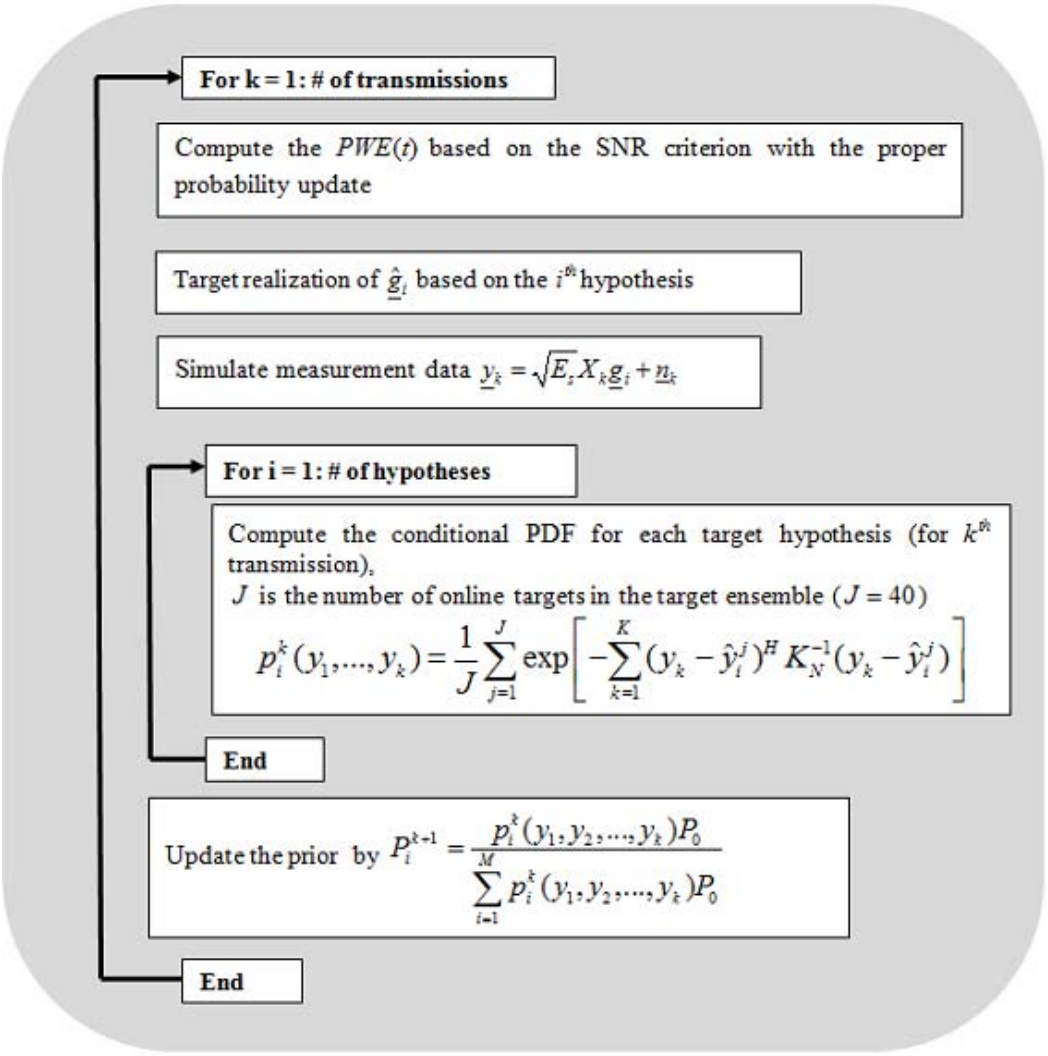

Figure 6. The pseudo-code block diagram of one radar classification evolution.

system by randomizing the key variables in the experiment. By simulating many realizations of every random variable in the experiment, the Monte Carlo simulation will have a classification performance result that is very close to the true performance of the system. The pseudo code for the Monte Carlo simulation is presented in Figure 7. The Monte Carlo simulation computes the probability of correct classification (P_{cc}) for the CR system at a specific transmission energy level E_s. For this particular energy constraint level, the simulation first chooses one target hypothesis and generates X number of target realizations based on this particular target hypothesis. Secondly, for each target

realization, the system generates Y measurement noise realizations. Third, for each noise realization, the system then performs one cycle of target classification and records the P_{cc} of the classification result. Next, the system averages the P_{cc} of the classification results for this one hypothesis. The system repeats the same procedure for the rest of the target hypotheses and averages the P_{cc} from all hypotheses to obtain the P_{cc} for this one particular energy level.

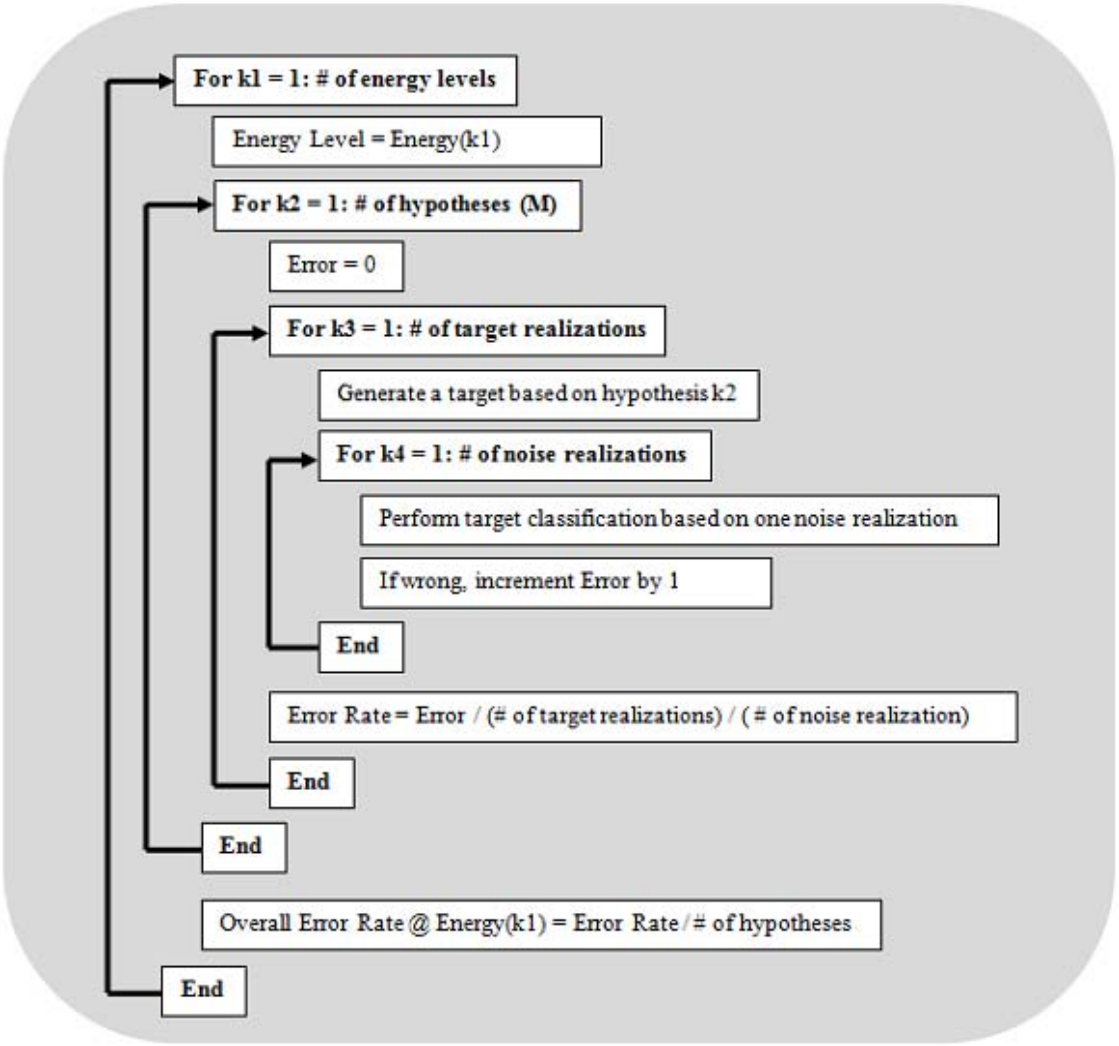

Figure 7. An example of the Monte Carlo simulation used in the experiment.

For the overall experiment, the Monte Carlo simulation system uses $X = 50$ for the number of target realizations and $Y = 10$ for the number of noise realizations. The energy levels E_s for this research are defined on a logarithmic scale ranged from 10^{-2} to 10 energy units. At the end, an overall P_{cc} vs. energy curve is plotted to evaluate the performance of the CR system.

For comparison purposes, this research also uses a traditional wideband pulse as the input illumination waveform to conduct the same experiments as the PWE waveform design method. An overall P_{cc} vs. energy curve is plotted for the wideband illumination waveform and uses this result as a benchmark to show the improvement of the SNR-based PWE waveform method.

The experimental setup for this research was explained in this chapter. This includes the method for target simulation, matched waveform design, target classification scheme implementation, and the Monte Carlo simulation setup for test evaluations. In the next chapter, a representative example the PWE waveform, the simulated targets and the results from various test runs are presented and explained.

VI. EXPERIMENTAL RESULTS

In order to test the algorithm presented in this research, a series of experiments were carried out to evaluate its performance. In this chapter, first, a representative example of a PWE illumination waveform is presented. Then, the test results of the experiments are presented along with detail explanations and conclusions.

A. REPRESENTATIVE EXAMPLE OF A PWE ILLUMINATION WAVEFORM

For the purpose of illustrating the PWE illumination process, a representative example is presented in this section. First, the proposed PSVs of the four target hypotheses are created using the parameters listed in Table 1. The proposed PDFs for the target to draw samples from are exponential PDFs with μ=2. The parameters for the PSVs are μ and σ, where μ defines the center frequencies of the energy bands of the targets and σ defines the relative amplitudes and bandwidths of the band-pass waveform spectra. The number of data samples used in this test is set to 64.

Table 1. Key parameters for the target hypotheses in the example.

Target Hypotheses	Target PDFs (PDF parameters)	μ	σ
Target # 1	Complex Exponential ($\mu = 2$)	0.15	0.01
Target # 2	Complex Exponential ($\mu = 2$)	0.2	0.015
Target # 3	Complex Exponential ($\mu = 2$)	0.25	0.02
Target # 4	Complex Exponential ($\mu = 2$)	0.3	0.025

The PSVs of the four target hypotheses are illustrated in Figure 8. By putting the four PSVs on one plot, we can see that none of the target spectra completely overlap any of the other target spectra. All target hypotheses have different amplitudes and bandwidths in their PSVs.

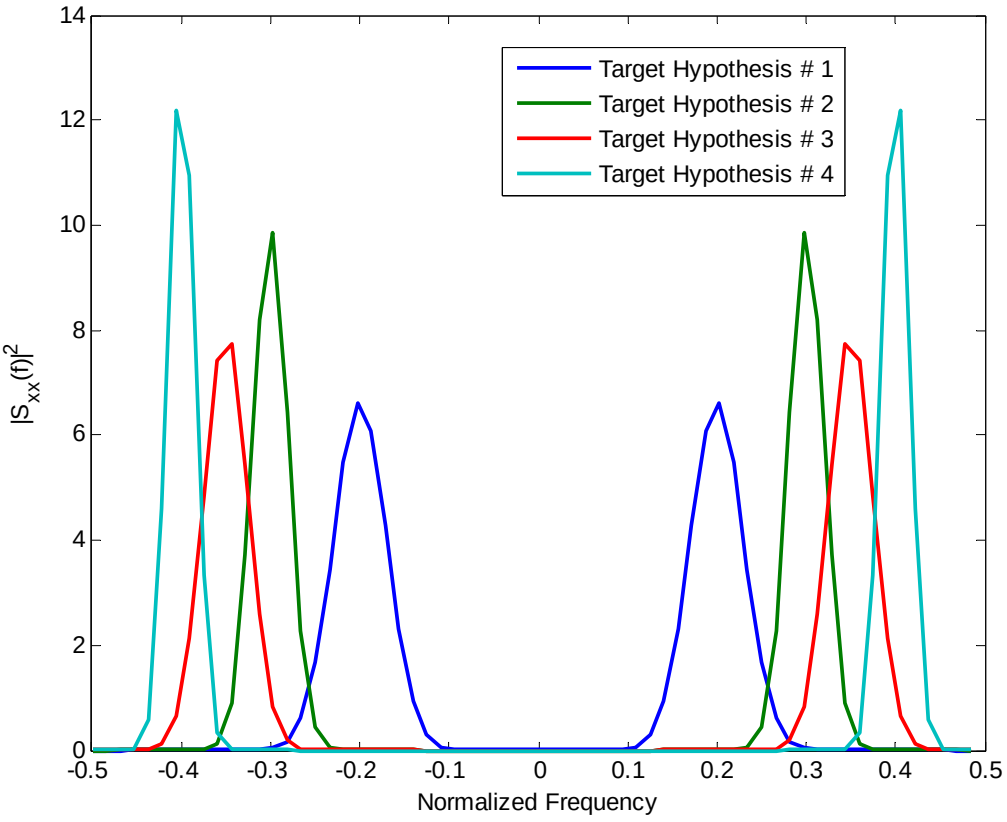

Figure 8. PSVs corresponding to the four target hypotheses.

Next, a particular target realization from target hypothesis H_1 is generated. The PSV of this target realization is illustrated in Figure 9. Because the experiment only sets the number of samples to 64, the PSV of any stochastic target realization is not very smooth in nature. However, the generated target still possesses the general properties of the target hypothesis in terms of total energy and band-pass frequencies. The target in Figure 9 and target hypothesis H_1 in Figure 8 both have center frequency 0.2 unit on a normalized frequency scale. The total energy of both PSVs is equal to 1 energy unit.

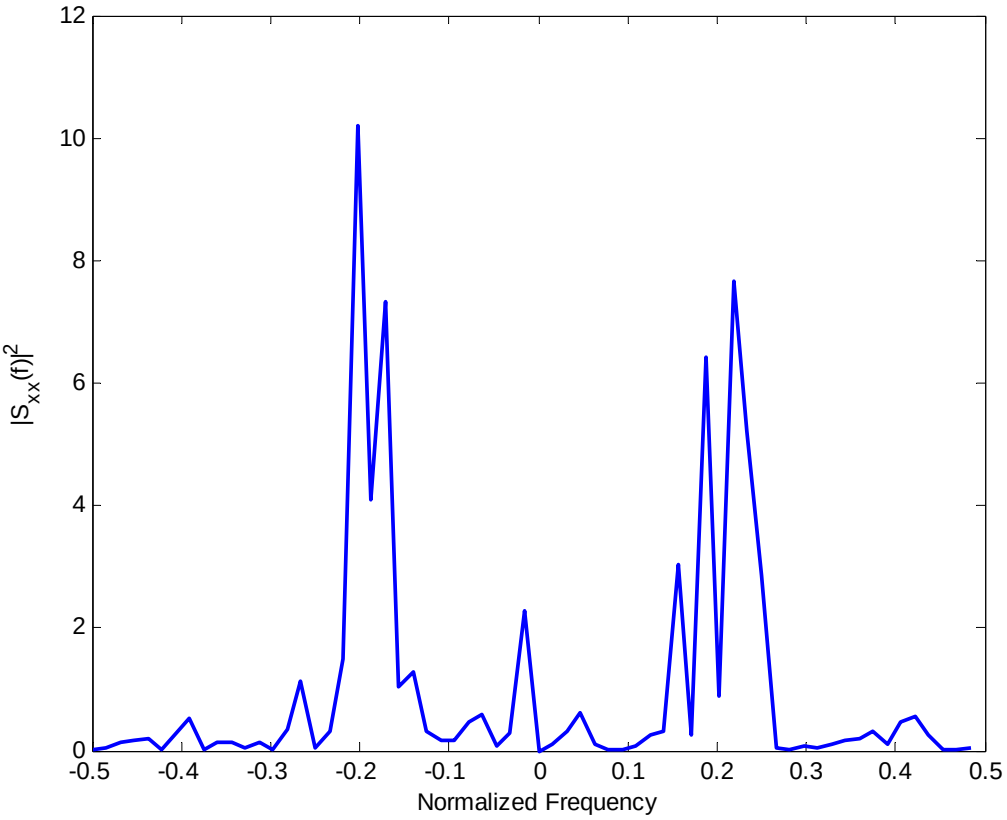

Figure 9. PSV of one target realization (Target Hypothesis # 1).

The PWE illumination waveform is created by the method described in the experimental setup. The PSVs of the first and the tenth illumination waveforms for both the PWE illumination waveform and the wideband illumination waveforms are illustrated in Figure 10. From the PSV plots we can see that for the initial transmission, the PWE illumination waveform possesses the properties of all four target hypotheses. Then, at the tenth transmission, the PWE waveform converges and focuses all of its energy towards the frequency bands in which target hypothesis H_1 resides. The wideband method stays the same for all ten transmissions. From this example, we can see that using the PWE illumination waveforms results in a very efficient distribution of the limited illumination energy toward the high energy parts of the PSV. When a wideband pulse is used, most energy is wasted on the frequency bands where the target spectra have very little or zero energy.

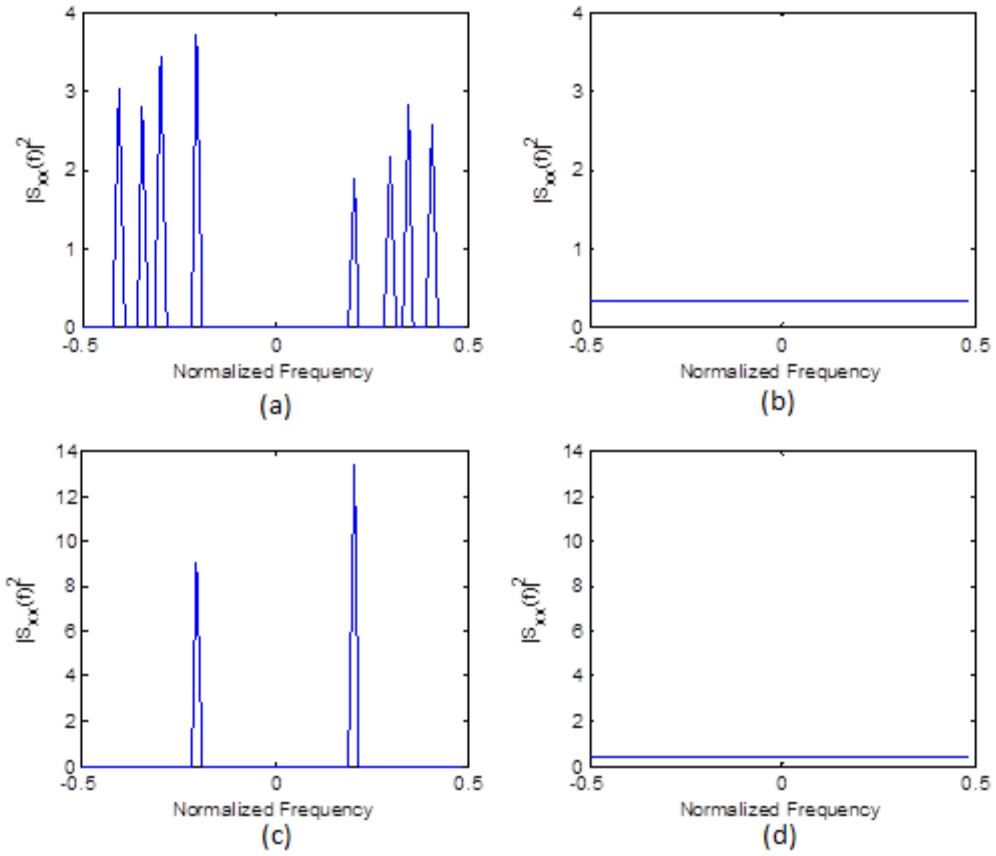

Figure 10. The initial and tenth transmission snapshots of the PSVs for PWE illumination waveform and the wideband illumination waveform: (a) PSV of the initial PWE illumination waveform; (b) PSV of the initial wideband illumination waveform; (c) PSV of the tenth PWE illumination waveform; (d) PSV of the tenth wideband illumination waveform.

The time waveforms of the PWE illumination waveform at the tenth transmission are illustrated in Figure 11. From the time waveforms of the real and imaginary values in the PWE illumination waveform, we can see a rough looking weighted sum of sinusoidal waveforms. This corresponds to the fact that the PWE waveforms are generated based on an eigenfunction solution, which produces sinusoidal functions.

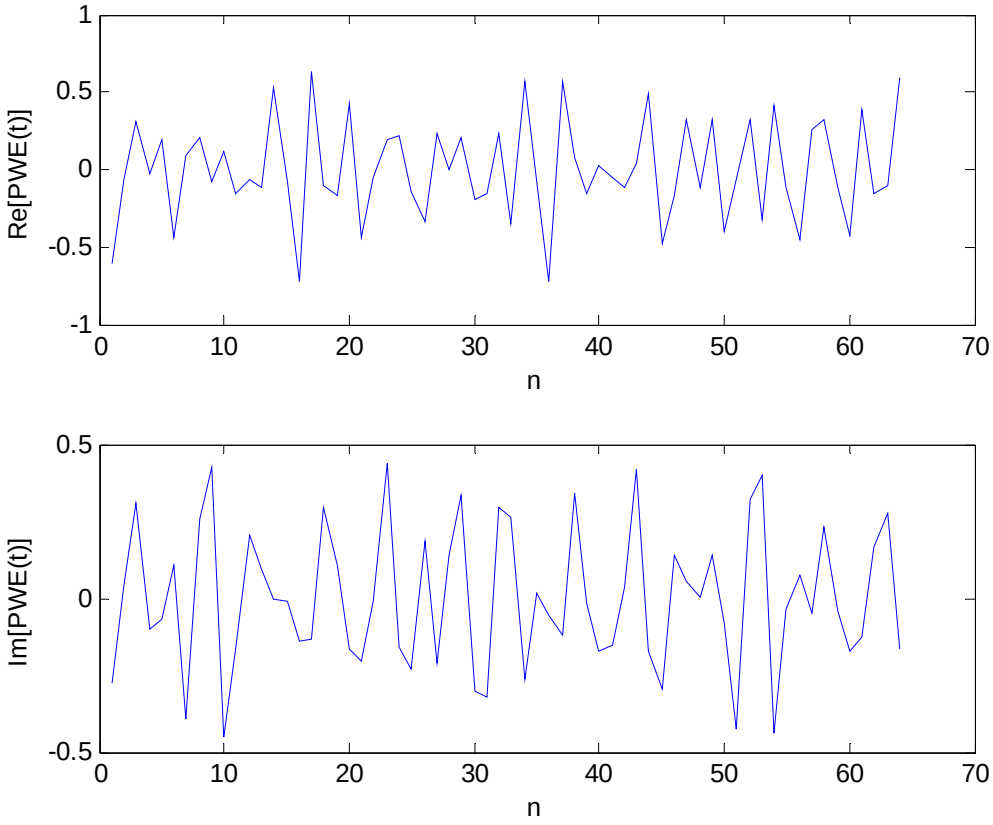

Figure 11. Time waveform of the PWE illumination waveform at the 10th transmission. Top and bottom are the real values and imaginary values of the PWE illumination waveform, respectively.

This concludes the demonstration of the PWE illumination waveform process. Next, the experimental results from various tests are presented and explained.

B. CLASSIFICATION RESULTS FOR FOUR GAUSSIAN TARGET CLASSES

The first experimental test set consists of four Gaussian distributed complex targets with different PSVs. This test is conducted mainly to evaluate the performance of the new classification algorithm on Gaussian target classes. The four proposed PSVs are illustrated in Figure 12. Each PSV is a mixture of two Gaussian distribution functions.

None of the target PSVs completely overlaps other target PSVs. The number of data samples used in this test is set to 64. The specific parameters of the four different target hypotheses are listed in Table 2.

Table 2. Parameter setup of the four target hypotheses for the first experiment.

Target Hypotheses	Target PDFs (PDF parameters)	μ	σ
Target # 1	Complex Gaussian $(\mu = 0, \sigma = 1)$	0.15	0.01
Target # 2	Complex Gaussian $(\mu = 0, \sigma = 1)$	0.2	0.015
Target # 3	Complex Gaussian $(\mu = 0, \sigma = 1)$	0.25	0.02
Target # 4	Complex Gaussian $(\mu = 0, \sigma = 1)$	0.3	0.025

The parameter μ defines the band-pass center frequencies of the PSVs, and the parameter σ defines the relative amplitudes and bandwidths of the energy bands of the PSVs.

An example of one set of target realizations based on the proposed PDFs and PSVs is illustrated in Figure 13. Because the experiment only has the number of samples set to 64, the spectrum of any stochastic target realization is not smooth in nature. However, the generated target still possesses the general properties of the target hypothesis proposed in Figure 12 in terms of total energy and band-pass frequencies. The spectra presented in Figure 13 conform to the respective PSVs of the target hypotheses.

The PDF estimates of one set of target realizations based on the proposed PDFs and PSVs are illustrated in Figure 14. The PDF estimates are computed using a univariate Kernel Density Estimator (KDE) as described in [19]. The PDFs of both the real and imaginary values in all four targets have a rough looking Gaussian shape with zero mean and unity variance, which conform to the proposed Gaussian PDF.

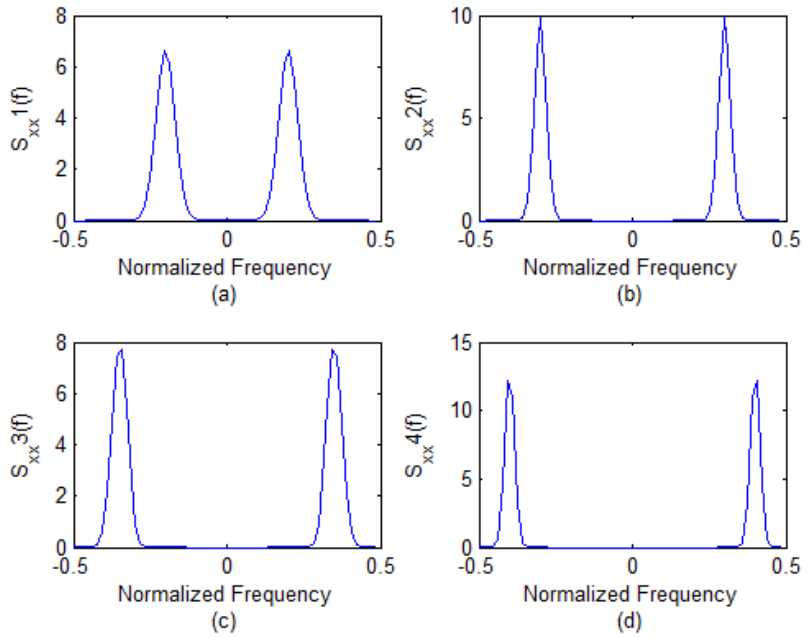

Figure 12. An example of the proposed PSVs of four target hypotheses: (a) target hypothesis one; (b) target hypothesis two; (c) target hypothesis three; (d) target hypothesis four.

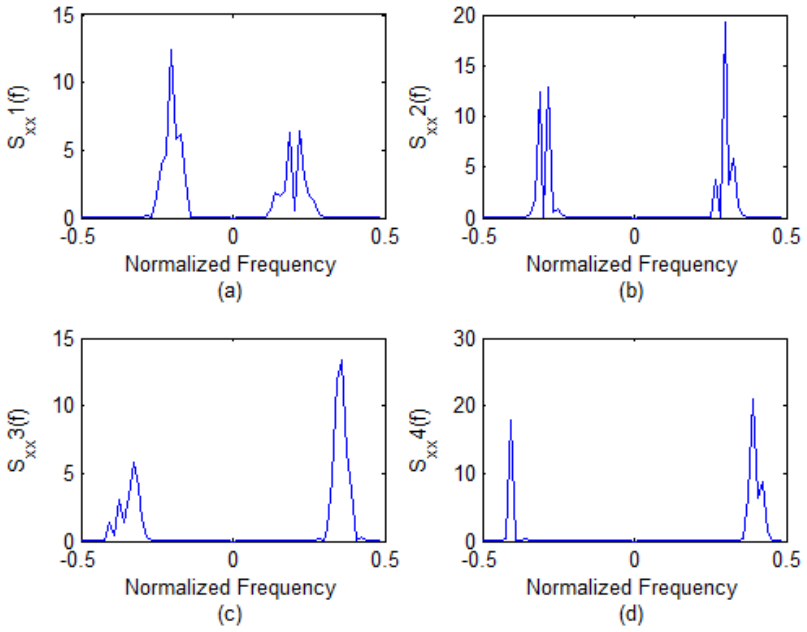

Figure 13. The spectra of one realization of targets from the first target hypothesis set based on four proposed PSVs and a Gaussian PDF: (a) target hypothesis one; (b) target hypothesis two; (c) target hypothesis three; (d) target hypothesis four.

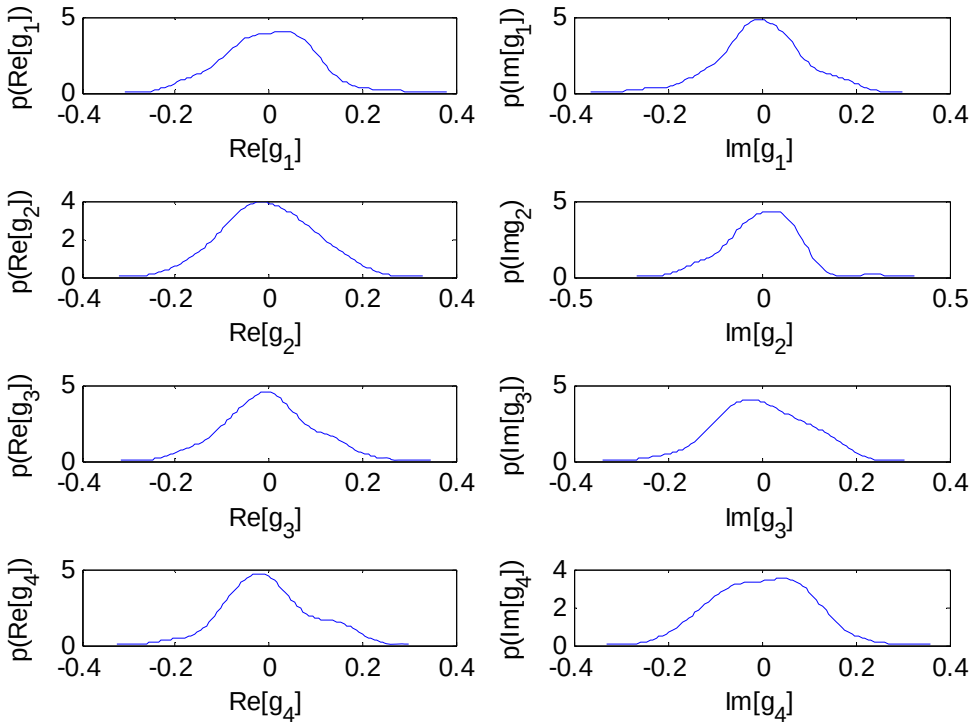

Figure 14. PDF estimates of the four target realizations. The PDF estimates of the real values of the four target realizations are presented on the left column and the PDF estimates of the imaginary values of the four target realizations are presented on the right column.

The time waveforms of one set of target realizations are illustrated in Figure 15. From the time waveforms, we can see the correlations in the data samples, which also indicate that the data samples in these targets are not independent due to the ZMNL transformation process.

The normal distribution plots of the first two targets from one set of target realizations are presented in Figure 16. The normal distribution plot is used for evaluating the Gaussianity of a signal. If the data samples in a signal are Gaussian distributed, then the data samples align to the red diagonal line in the normal distribution plot. From these normal distribution plots, we can see that the data samples from first two target realizations are approximately Gaussian distributed.

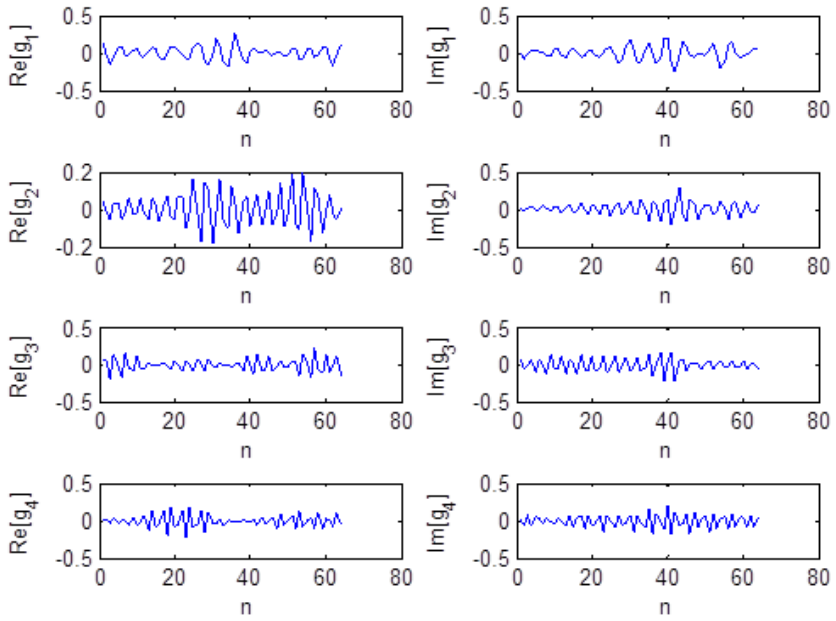

Figure 15. Time waveform of the four target hypotheses. Left column: real values of target realizations; right column: imaginary values of the target realizations.

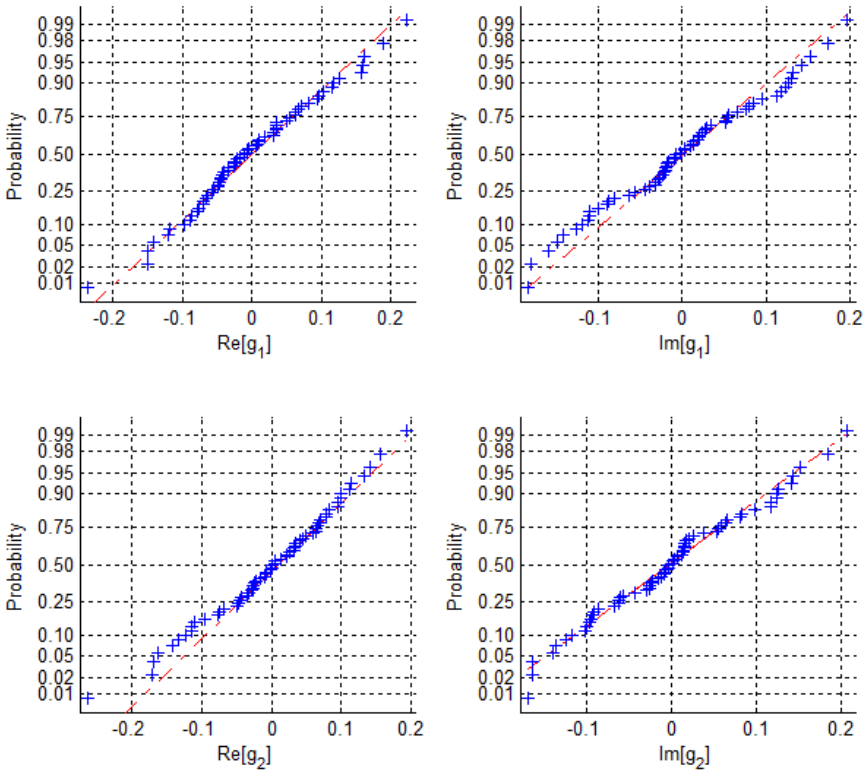

Figure 16. Normal distribution plots of the first two targets in the target realization set. Left column: normal distribution plots of the real values of the first two targets; right column: normal distribution plots of the imaginary values of the first two targets.

The normal distribution plots of the last two targets from one set of target realizations are presented in Figure 17. From these normal distribution plots, we see that the data samples from last two target realizations are approximately Gaussian distributed.

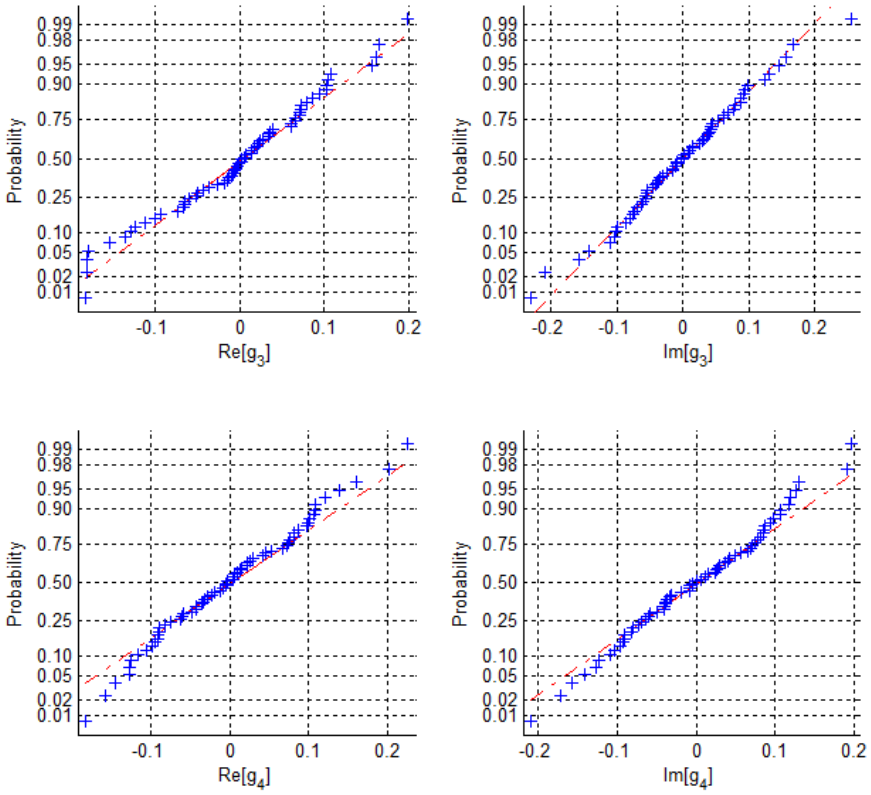

Figure 17. Normal distribution plots of the first two targets in the target realization set. Left column: normal distribution plots of the real values of the first two targets; right column: normal distribution plots of the imaginary values of the first two targets.

The Monte Carlo experimental result for one radar transmission is presented in Figure 18. The Monte Carlo simulation is set to generate 50 target realizations and ten noise realizations for each target realization. The number of the online target realizations for the expected value estimation is set to $N_g = 40$. For four target hypotheses that are Gaussian distributed, the PWE illumination waveform outperforms the traditional wideband illumination waveform and saves approximately 6 dB in transmission energy when the P_{cc} is 90%. Another way to view the performance gain is that for a given mid-

range transmission energy, we achieve approximately a 100% increase in P_{cc}. At very low energy levels, the receiver can no longer obtain any useful information from the received data since the AWGN in the receiver becomes the dominant component. At very high energy levels, any waveform is a good waveform; thus, the wideband illumination waveform is just as good as the PWE illumination waveform.

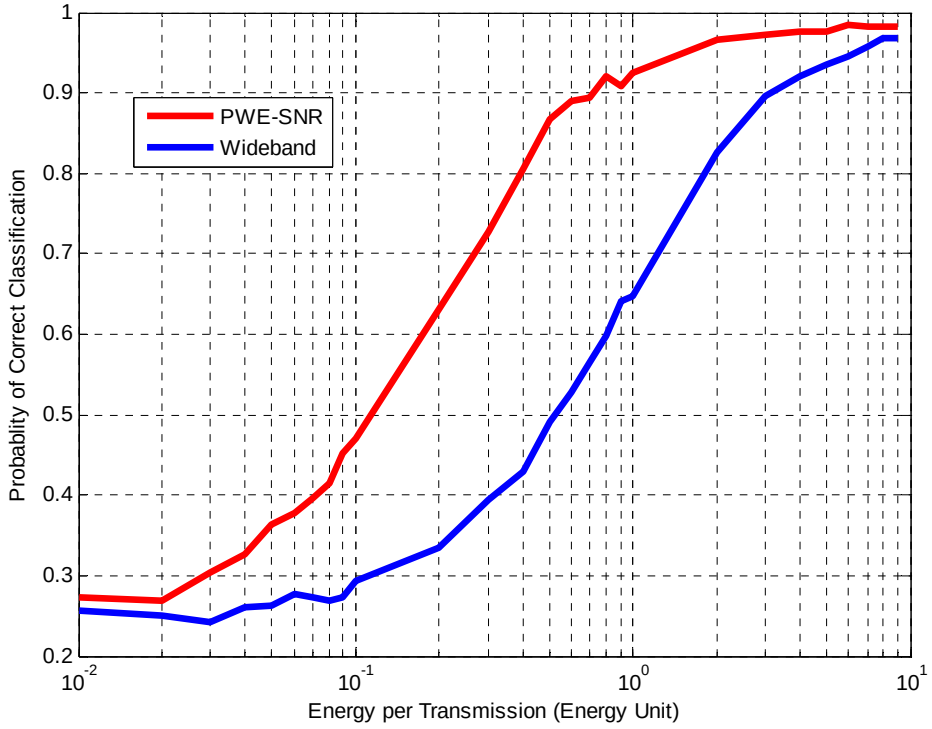

Figure 18. Classification performance curves of the optimized SNR illumination waveform and a traditional wideband waveform with the implementation of the NGCCR system for one transmission. Target distributions: Gaussian x 4. Monte Carlo setup: 50 target realizations; ten noise realizations. NGCCR system setup: 40 online target realizations for the ensemble averaging.

The Monte Carlo experimental result for ten transmissions is presented in Figure 19. The Monte Carlo simulation is set to generate 50 target realizations and ten noise realizations for each target realization. The number of the online target realizations for the expected value estimation is set to $N_g = 40$. The P_{cc} for both illumination waveforms have improved in this case. For four target hypotheses that are Gaussian distributed, the PWE illumination waveform outperforms the traditional wideband illumination

waveform and saves approximately 5 dB in transmission energy when the P_{cc} is 90%. Another way to view the performance gain is that for a given mid-range transmission energy, we achieve approximately a 100% increase in P_{cc}. At very low energy levels, the receiver can no longer obtain any useful information from the received data since the AWGN in the receiver is the dominant component. At very high energy levels, the wideband illumination waveform has a 100% P_{cc}. However, the PWE illumination waveform only has a near 100% P_{cc}. One of the reasons may be that more Monte Carlo averaging is needed. For the majority of the time, the PWE illumination waveform is still the better choice.

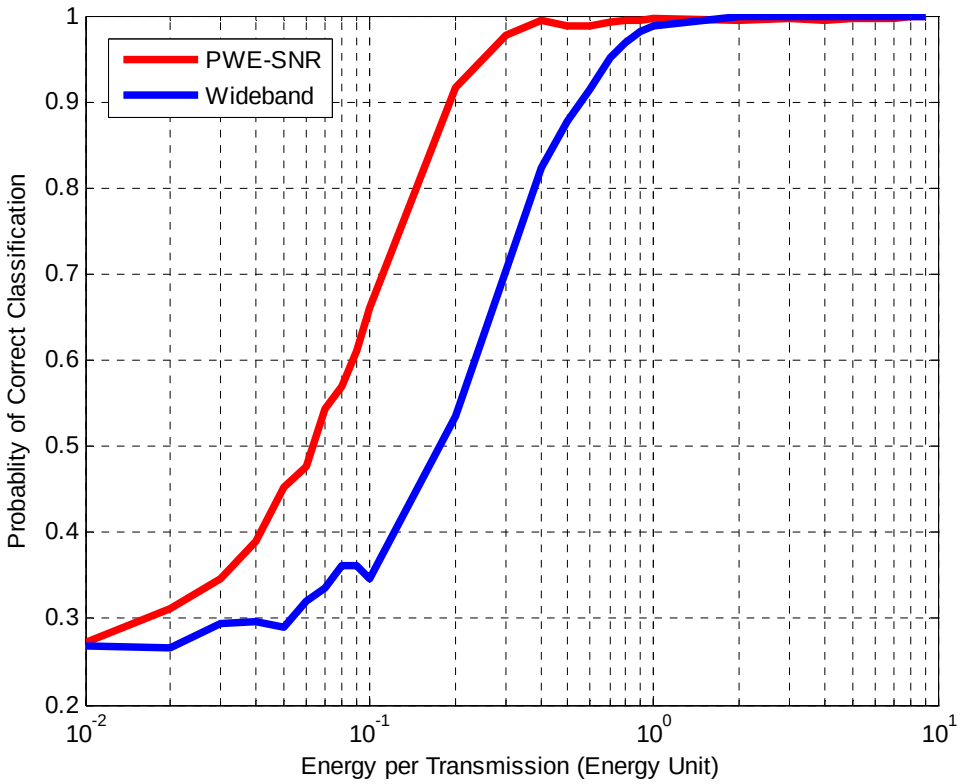

Figure 19. Classification performance curves of the optimized SNR illumination waveform and a traditional wideband waveform with the implementation of the NGCCR system for ten transmissions. Target distributions: Gaussian x 4. Monte Carlo setup: 50 target realizations; ten noise realizations. NGCCR system setup: 40 online target realizations for the ensemble averaging.

C. CLASSIFICATION RESULTS FOR FOUR EXPONENTIAL TARGET CLASSES

The second experimental test set consists of four exponentially distributed complex targets with different PSVs. This test is conducted mainly to evaluate the performance of the new classification algorithm on non-Gaussian target classes. The four proposed PSVs are illustrated in Figure 20. Each PSV is a mixture of two Gaussian distribution functions. None of the target PSVs completely overlaps other target PSVs. The number of data samples used in this test is set to 64. The specific parameters of the four different target hypotheses are listed in Table 3.

Table 3. Parameter setup of the four target hypotheses for the second experiment.

Target Hypotheses	Target PDFs (PDF parameters)	μ	σ
Target # 1	Complex Exponential ($\mu = 2$)	0.15	0.01
Target # 2	Complex Exponential ($\mu = 2$)	0.2	0.015
Target # 3	Complex Exponential ($\mu = 2$)	0.25	0.02
Target # 4	Complex Exponential ($\mu = 2$)	0.3	0.025

The parameter μ defines the band-pass center frequencies of the PSVs, and the parameter σ defines the relative amplitudes and bandwidths of the energy bands of the PSVs.

An example of one set of target realizations based on the proposed PDFs and PSVs is illustrated in Figure 21. Because the experiment only has 64 samples, the spectrum of any stochastic target realization is not very smooth in nature. However, the generated target still possesses the general properties of the target hypothesis proposed in Figure 20 in terms of total energy and band-pass frequencies. The spectra presented in Figure 21 conform that the targets possess the proposed PSVs of the target hypotheses.

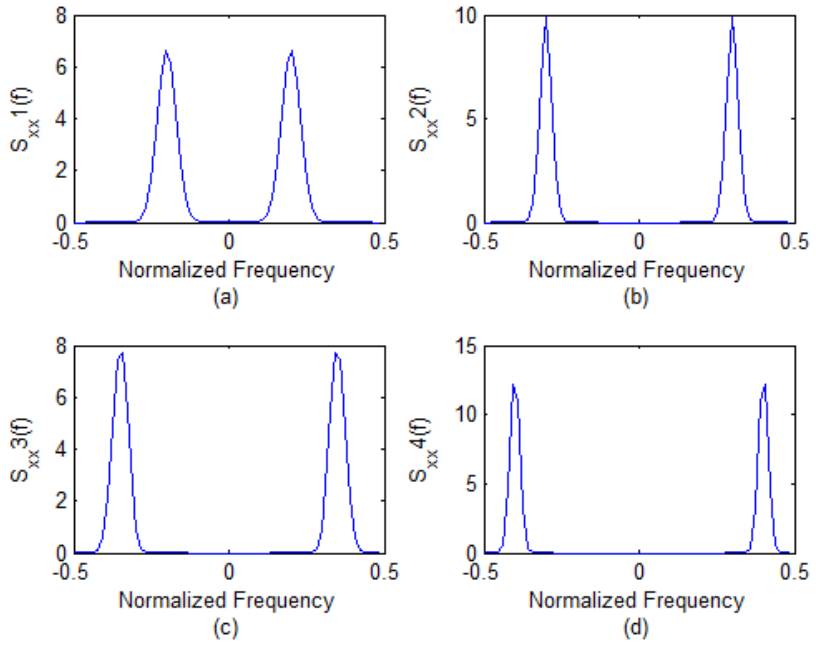

Figure 20. The four proposed PSVs for the target hypotheses in the second experimental test set: (a) target hypothesis one; (b) target hypothesis two; (c) target hypothesis three; (d) target hypothesis four.

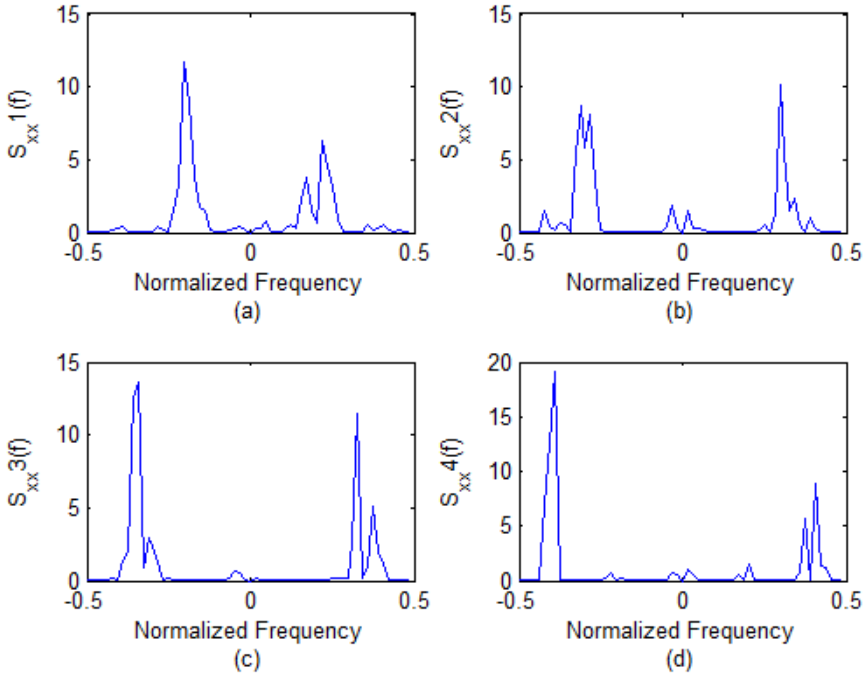

Figure 21. The spectra of one realization of targets from the first target hypothesis set based on four proposed PSVs and an Exponential PDF: (a) target hypothesis one; (b) target hypothesis two; (c) target hypothesis three; (d) target hypothesis four.

The PDF estimates of one set of target realizations based on the proposed PDFs and PSVs are illustrated in Figure 22. The PDFs of both the real and imaginary values in all four target realizations have a rough looking exponential distribution with parameter $\mu = 2$, which conforms to the proposed exponential PDF.

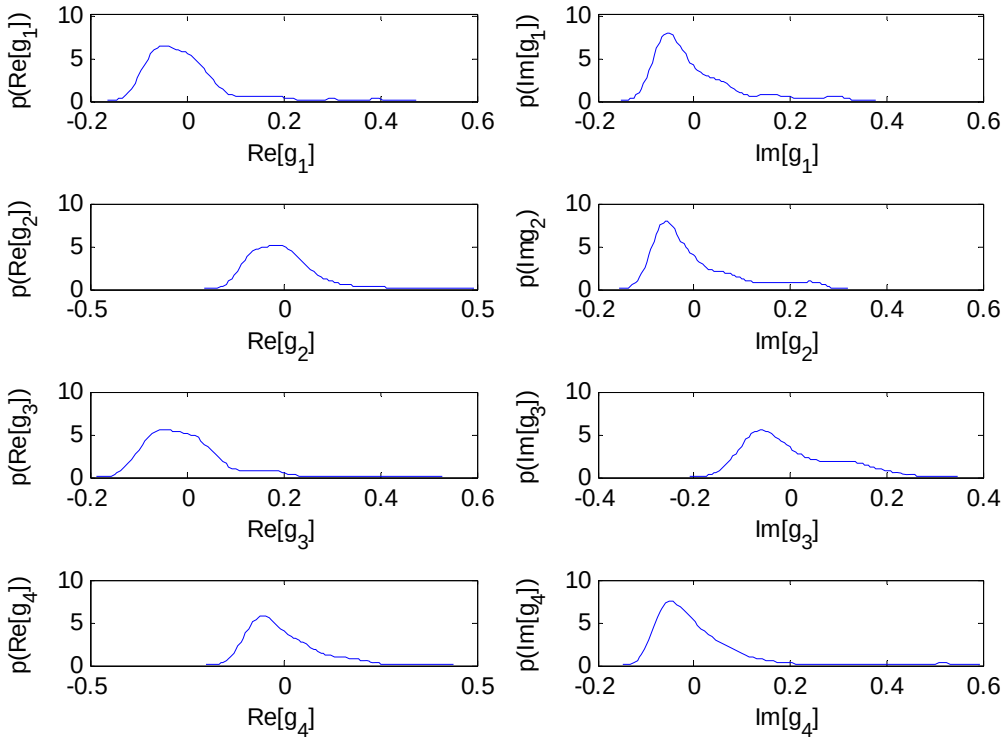

Figure 22. PDF estimates of one particular realization of the second target hypothesis set. The four targets are exponentially distributed. The real values of the targets are presented on the left column and the imaginary values of the targets are presented on the right column.

The time waveforms of one set of target realizations are illustrated in Figure 23. From the time waveforms, we can see the correlation in the data samples, which also indicate that the data samples in these targets are not independent due to the ZMNL transformation process.

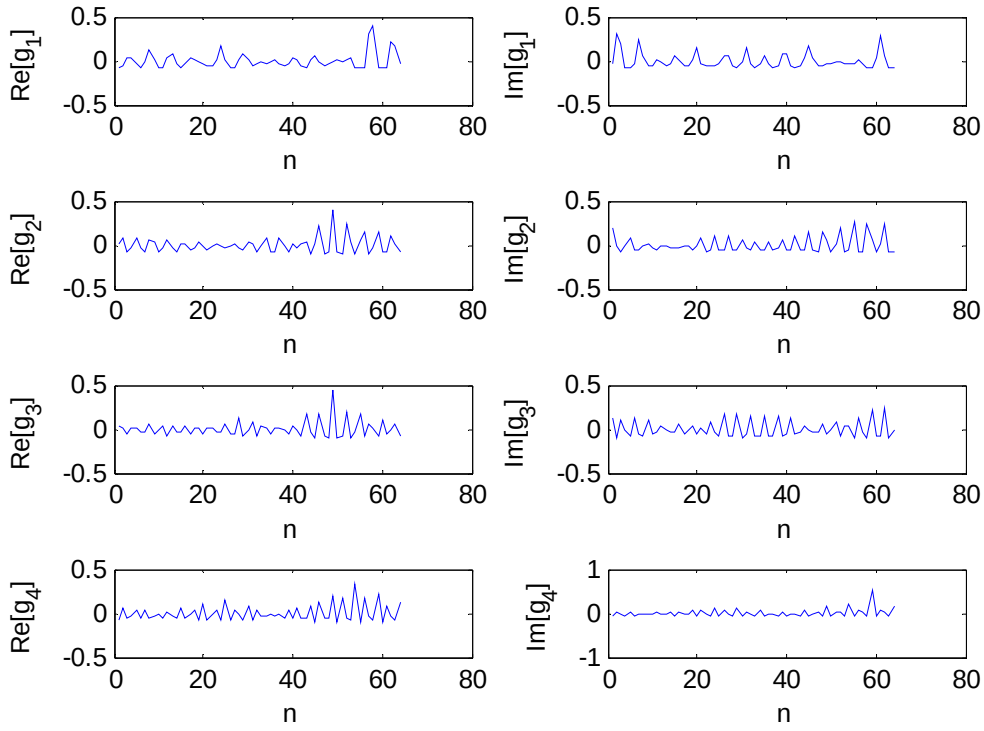

Figure 23. Time waveforms of one particular realization of the second target hypothesis set. The real values of the targets are presented on the left column and the imaginary values of the targets are presented on the right column.

The normal distribution plots of the first two targets from one set of target realizations are presented in Figure 24. From these normal distribution plots, we can see that the data samples do not align with the red diagonal line in the normal distribution plot, which implies that first two targets realizations are not Gaussian distributed.

The normal distribution plots of the last two targets from one set of target realizations are presented in Figure 25. From these normal distribution plots, we can see that the data samples do not align with the red diagonal line in the normal distribution plot, which conforms that last two target realizations are not Gaussian distributed.

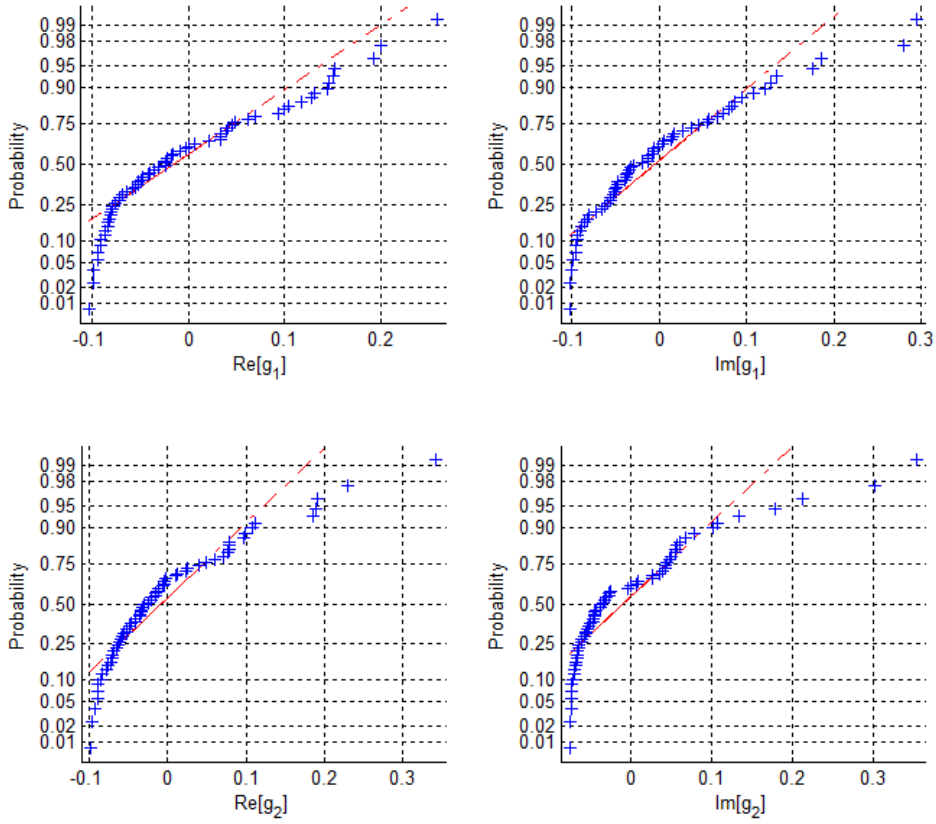

Figure 24. Normal distribution plot of one particular realization of the second target hypothesis set. The plots for the real values of the first two targets are presented on the left column and the plots for the imaginary values of the first two targets are presented on the right column.

The Monte Carlo experimental result for one radar transmission is presented in Figure 26. The Monte Carlo simulation is set to generate 50 target realizations and ten noise realizations for each target realization. The number of the online target realizations for the expected value estimation is set to $N_g = 40$. For four target hypotheses that are exponentially distributed, the PWE illumination waveform outperforms the traditional wideband illumination waveform by approximately 10 dB in transmission energy when P_{cc} is 90%. Another way to view the performance gain is that for a given mid-range transmission energy, we achieve approximately a 100% increase in P_{cc}. At very low energy levels, the receiver can no longer obtain any useful information from the received data since the AWGN in the receiver is the dominant component. At very high energy

levels, any waveform is a good waveform; thus, the wideband illumination waveform is just as good as the PWE illumination waveform at high energy levels.

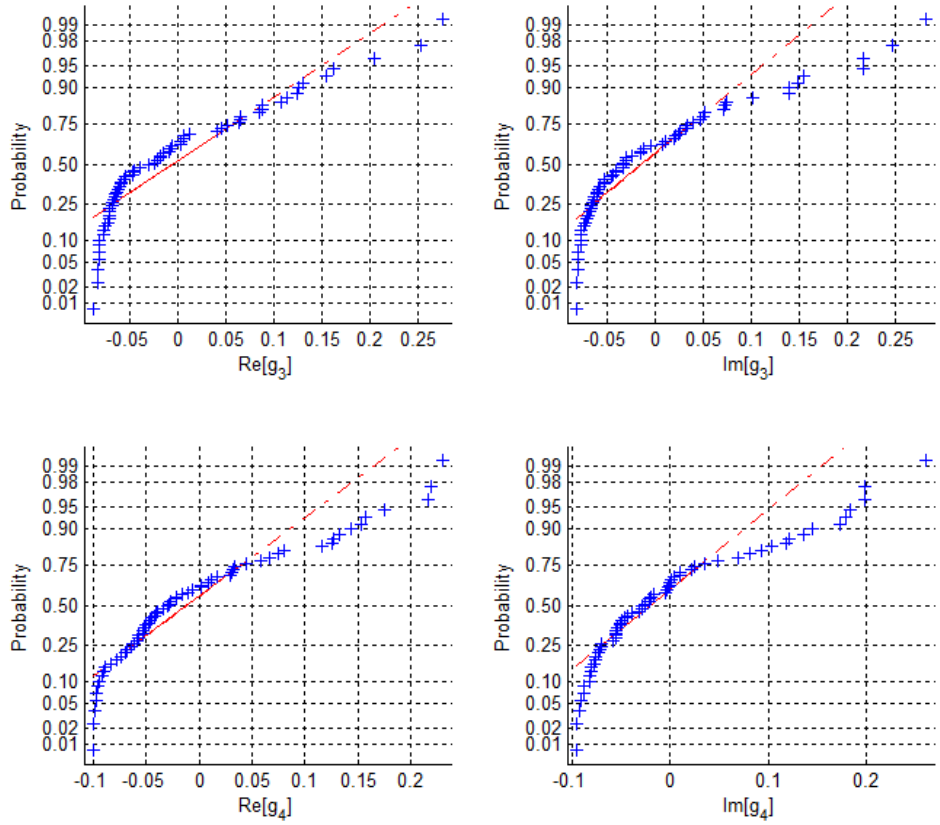

Figure 25. Normal distribution plot of one particular realization of the second target hypothesis set. The plots for the real values of the last two targets are presented on the left column and the plots for the imaginary values of the last two targets are presented on the right column.

The Monte Carlo experimental result for ten radar transmissions is presented in Figure 27. The Monte Carlo simulation is set to generate 50 target realizations and ten noise realizations for each target realization. The number of the online target realizations for the expected value estimation is set to $N_g = 40$. The P_{cc} for both illumination waveforms have improved in this case. For four target hypotheses that are exponentially distributed, the PWE illumination waveform outperforms the traditional wideband illumination waveform by approximately 4 dB in transmission energy when P_{cc} is 90%. Another way to view the performance gain is that for a given mid-range transmission

energy, we achieve approximately a 100% increase in P_{cc}. At very low energy levels, the receiver can no longer obtain any useful information from the received data since the AWGN in the receiver is the dominant component. At very high energy levels, the wideband illumination waveform has a 100% P_{cc}. However, the PWE illumination waveform only has a near 100% P_{cc}. One of the reasons may be that more Monte Carlo averaging is needed. For the majority of the time, the PWE illumination waveform is still the better choice. Also, the P_{cc} curves for the non-Gaussian distributed targets are very similar to the P_{cc} curves for the Gaussian distributed targets. This result shows the effectiveness of the NGCCR detection algorithm for classifying non-Gaussian targets.

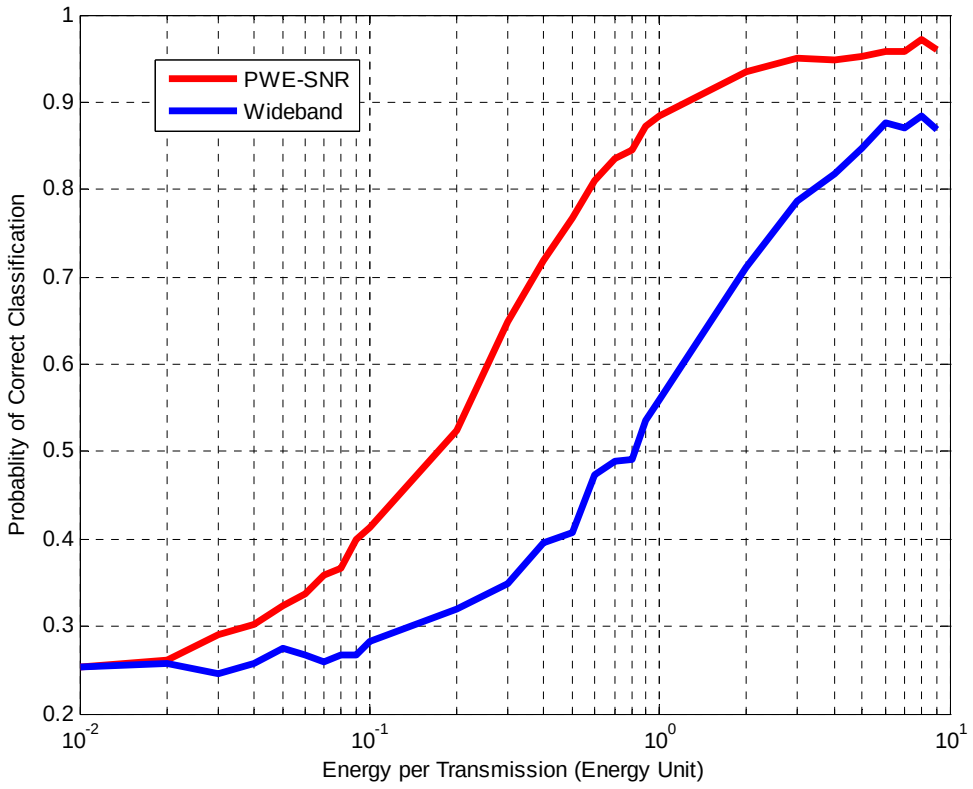

Figure 26. Classification performance curves of the optimized SNR illumination waveform and a traditional wideband waveform with the implementation of the NGCCR system for one transmission. Target distributions: exponential x 4. Monte Carlo setup: 50 target realizations; ten noise realizations. NGCCR system setup: 40 online target realizations for the ensemble averaging.

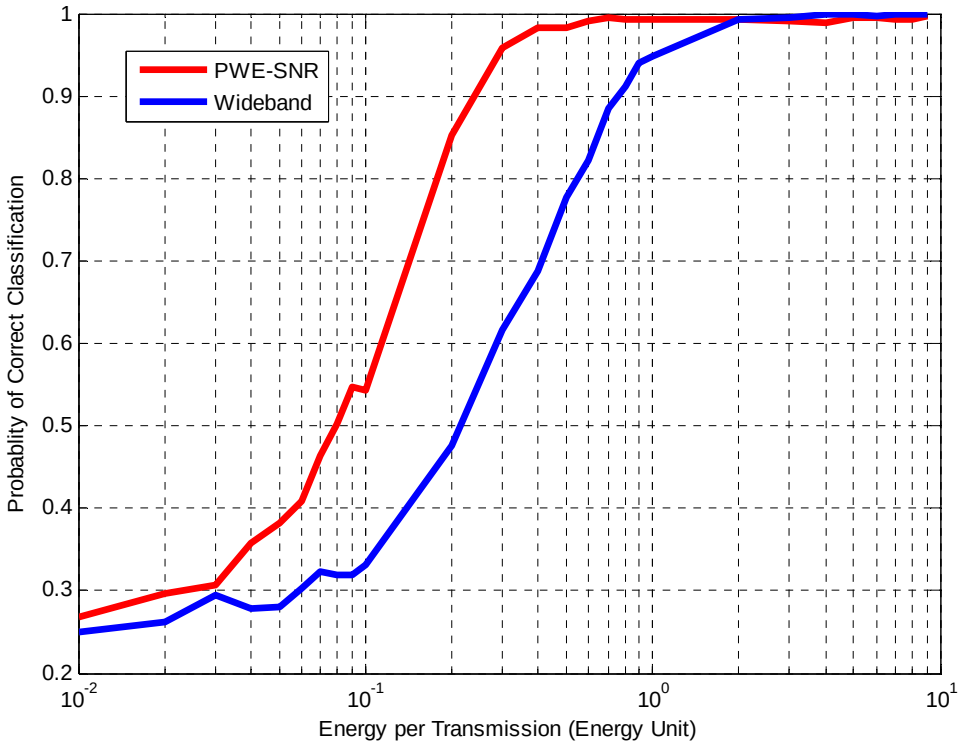

Figure 27. Classification performance curves of the optimized SNR illumination waveform and a traditional wideband waveform with the implementation of the NGCCR system for ten transmissions. Target distributions: exponential x 4. Monte Carlo setup: 50 target realizations; ten noise realizations. NGCCR system setup: 40 online target realizations for the ensemble averaging.

D. CLASSIFICATION RESULTS FOR FOUR NON-GAUSSIAN TARGET CLASSES

The last experimental test set consists of four non-Gaussian distributed complex targets with different PSVs. The non-Gaussian PDFs are Rayleigh, exponential, Gamma, and log-normal distributions. This test is conducted mainly to evaluate the performance of the new algorithm for non-Gaussian target classes with four different distributions. The four proposed PSVs are illustrated in Figure 28. Each PSV is a mixture of two Gaussian distribution functions. None of the target PSVs completely overlaps other target PSVs. The number of data samples used in this test is set to 64. The specific parameters of the four different target hypotheses are listed in Table 4.

Table 4. Parameter setup of the four target hypotheses for the third experiment.

Target Hypotheses	Target PDFs (PDF parameters)	μ	σ
Target # 1	Complex Rayleigh $(\sigma = 10)$	0.15	0.01
Target # 2	Complex Exponential $(\mu = 2)$	0.2	0.015
Target # 3	Complex Gamma $(k = 2, \theta = 2)$	0.25	0.02
Target # 4	Complex Log-Normal $(\mu = 0, \sigma = 1)$	0.3	0.025

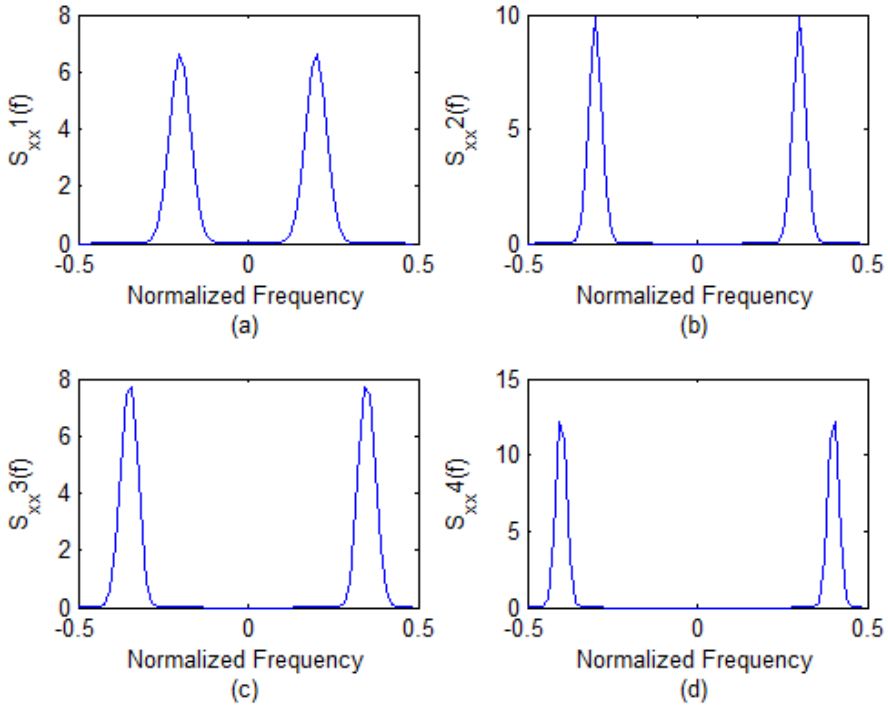

Figure 28. The four proposed PSVs for the target hypotheses in the last experimental test set: (a) target hypothesis one; (b) target hypothesis two; (c) target hypothesis three; (d) target hypothesis four.

The parameter μ defines the band-pass center frequencies of the PSVs, and the parameter σ defines the relative amplitudes and bandwidths of the energy bands of the PSVs.

An example of one set of target realizations based on the proposed PDFs and PSVs is illustrated in Figure 29. Because the experiment only has 64 samples, the spectrum of any stochastic target realization is not smooth in nature. However, the generated target still possesses the general properties of the target hypothesis proposed in Figure 28 in terms of total energy and band-pass frequencies. The spectra presented in Figure 29 conform with the specified PSVs of the target hypotheses.

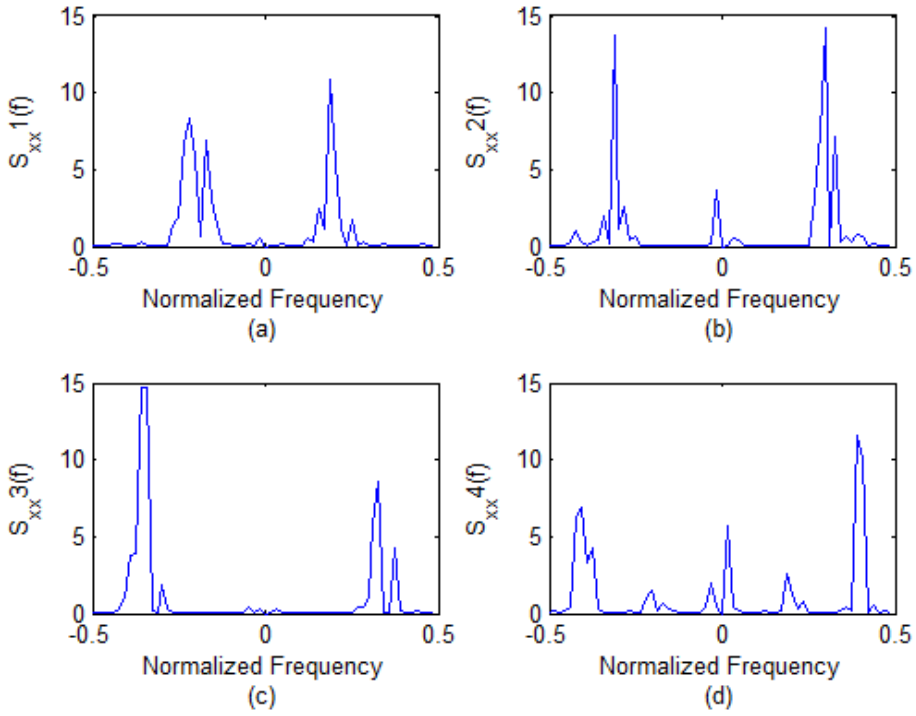

Figure 29. The spectra of one realization of targets from the first target hypothesis set based on four proposed PSVs and four different non-Gaussian PDFs: (a) target hypothesis one; (b) target hypothesis two; (c) target hypothesis three; (d) target hypothesis four.

The PDF estimates of one set of target realizations based on the proposed PDFs and PSVs are illustrated in Figure 30. The PDFs of both the real and imaginary values in the first target have a rough looking Rayleigh distribution with parameter $\sigma = 10$; the

PDFs of both the real and imaginary values in the second target have a rough looking Exponential distribution with parameter $\mu = 2$; the PDFs of both the real and imaginary values in the third target have a rough looking Gamma distribution with parameter $k = 2$ and $\theta = 2$; the PDFs of both the real and imaginary values in the fourth target have a rough looking Log-Normal distribution with parameter $\mu = 0$ and $\sigma = 1$. These PDF estimates show that these target realizations all approximate the proposed non-Gaussian PDFs.

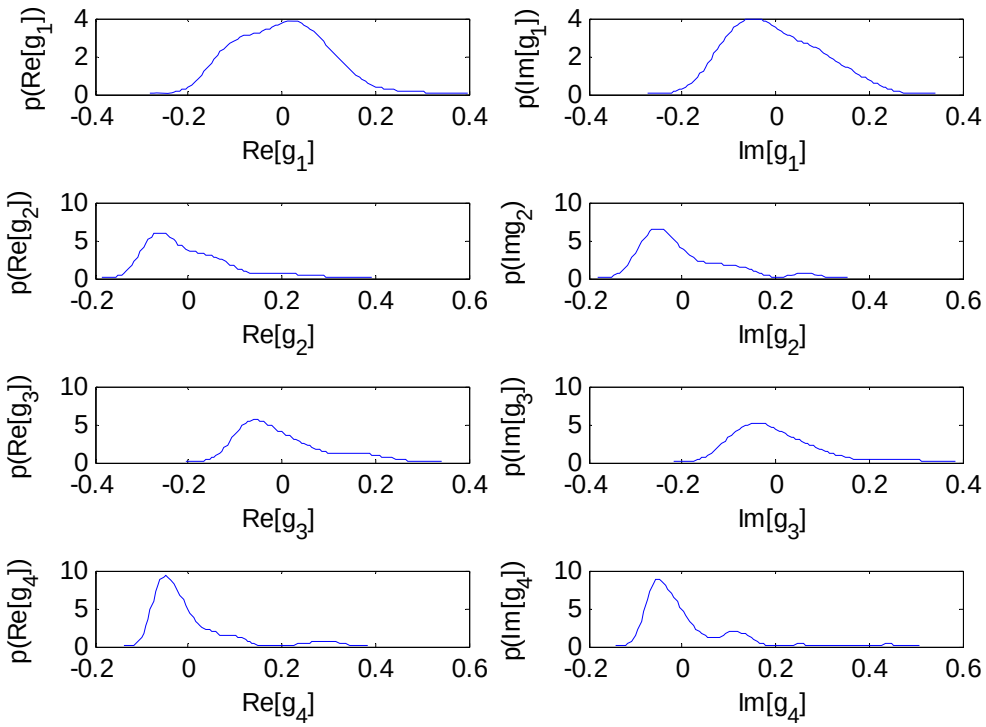

Figure 30. PDF estimates of one particular realization of the last target hypothesis set. The proposed PDFs for the four targets are Rayleigh, exponential, Gamma, and log-normal PDFs respectively. The real values of the targets are presented on the left column and the imaginary values of the targets are presented on the right column.

The time waveforms of one set of target realizations are illustrated in Figure 31. From the time waveforms, we can see the correlation in the data samples, which also indicate that the data samples in these targets are not independent due to the ZMNL transformation process.

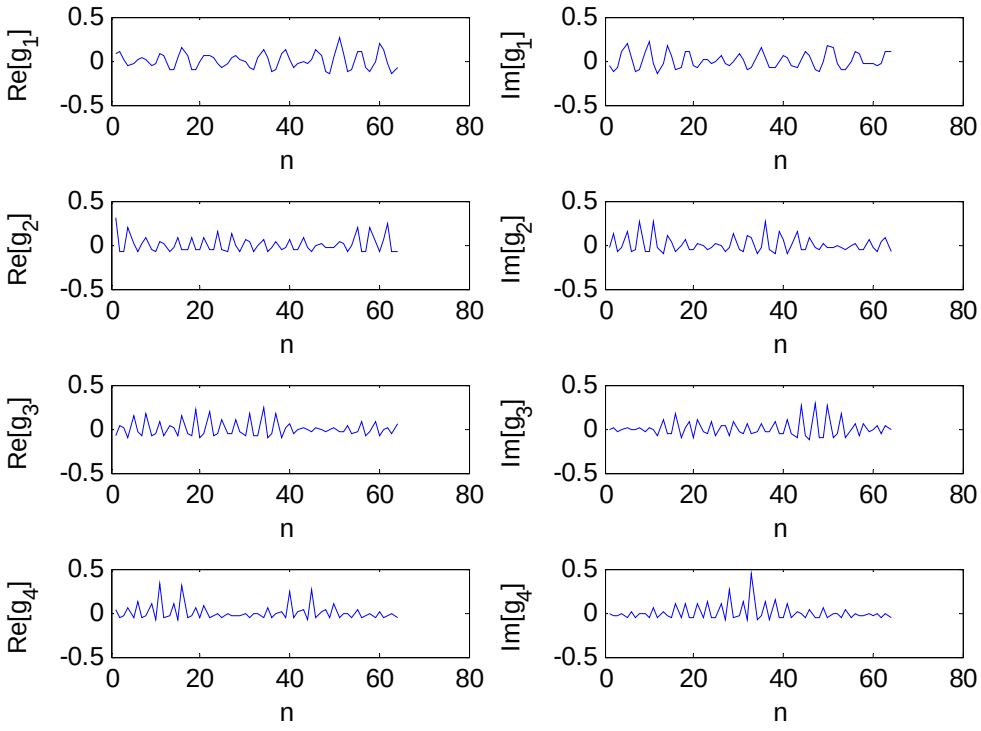

Figure 31. Time waveforms of one particular realization of the last target hypothesis set. The real values of the targets are presented on the left column and the imaginary values of the targets are presented on the right column.

The normal distribution plots of the first two targets from one set of target realizations are presented in Figure 32. From these normal distribution plots, we can see that the data samples do not align to the red diagonal line in the normal distribution plot, which confirms that first two target realizations are not Gaussian distributed.

The normal distribution plots of the last two targets from one set of target realizations are presented in Figure 33. From these normal distribution plots, we can see

that the data samples do not align to the red diagonal line in the normal distribution plot, which confirms that last two target realizations are not Gaussian distributed.

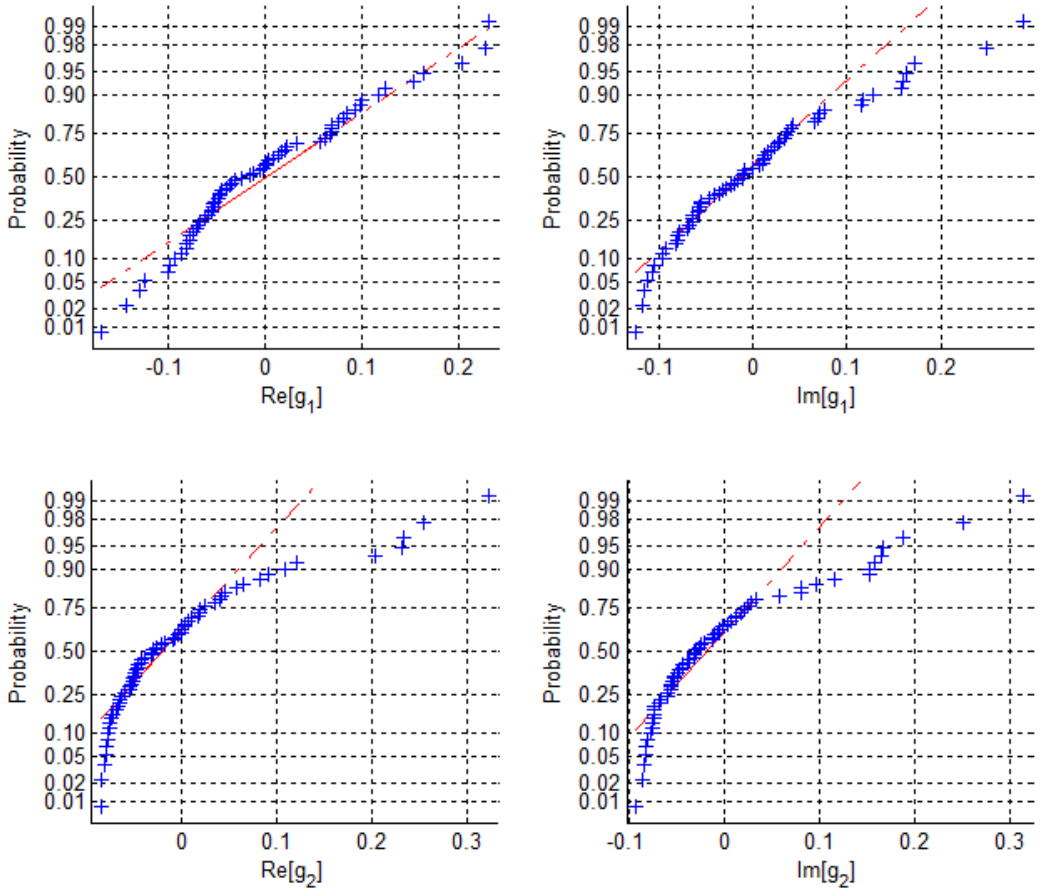

Figure 32. Normal distribution plot of one particular realization of the last target hypothesis set. The plots for the real values of the first two targets are presented on the left column and the plots for the imaginary values of the first two targets are presented on the right column.

The Monte Carlo experimental result for one radar transmission is presented in Figure 34. The Monte Carlo simulation is set to generate 50 target realizations and ten noise realizations for each target realization. The number of the online target realizations for the expected value estimation is set to $N_g = 40$. For four target hypotheses that are Rayleigh, exponential, Gamma, and log-normal distributed, respectively, the PWE illumination waveform outperforms the traditional wideband illumination waveform by approximately 6 dB in transmission energy when P_{cc} is 90%. Another way to view the

performance gain is that for a given mid-range transmission energy, we achieve approximately a 100% increase in P_{cc}. At very low energy levels, the receiver can no longer obtain any useful information from the received data since the AWGN in the receiver is the dominant component. At very high energy levels, any waveform is a good waveform; thus, the wideband illumination waveform is just as good as the PWE illumination waveform at high energy levels. Note that for this set of non-Gaussian targets, it appears that P_{cc} for the PWE waveform does not reach the 100% level after only one transmission (at least not over the range of energy levels plotted). However, after ten iterations, we see that the P_{cc} for the PWE waveform reaches 100% (see Figure 35).

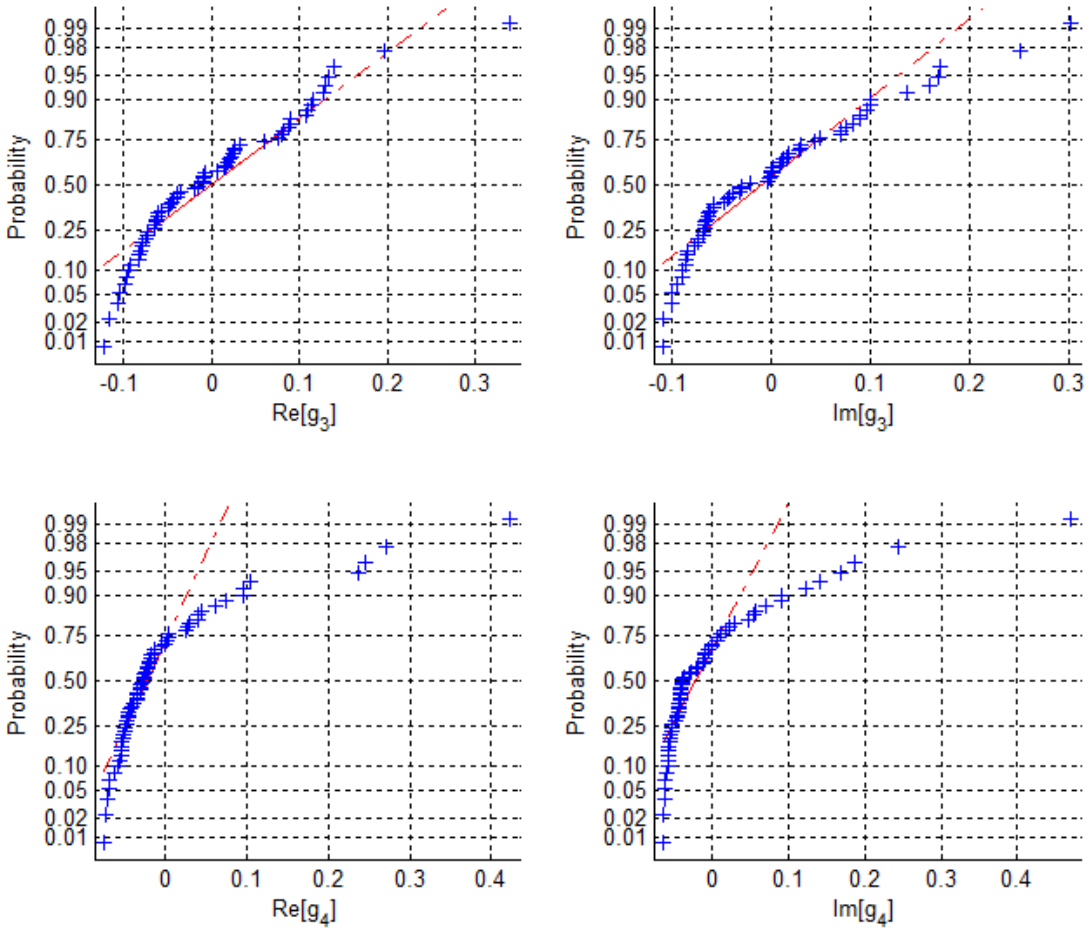

Figure 33. Normal distribution plot of one particular realization of the last target hypothesis set. The plots for the real values of the last two targets are presented on the

left column and the plots for the imaginary values of the last two targets are presented on the right column.

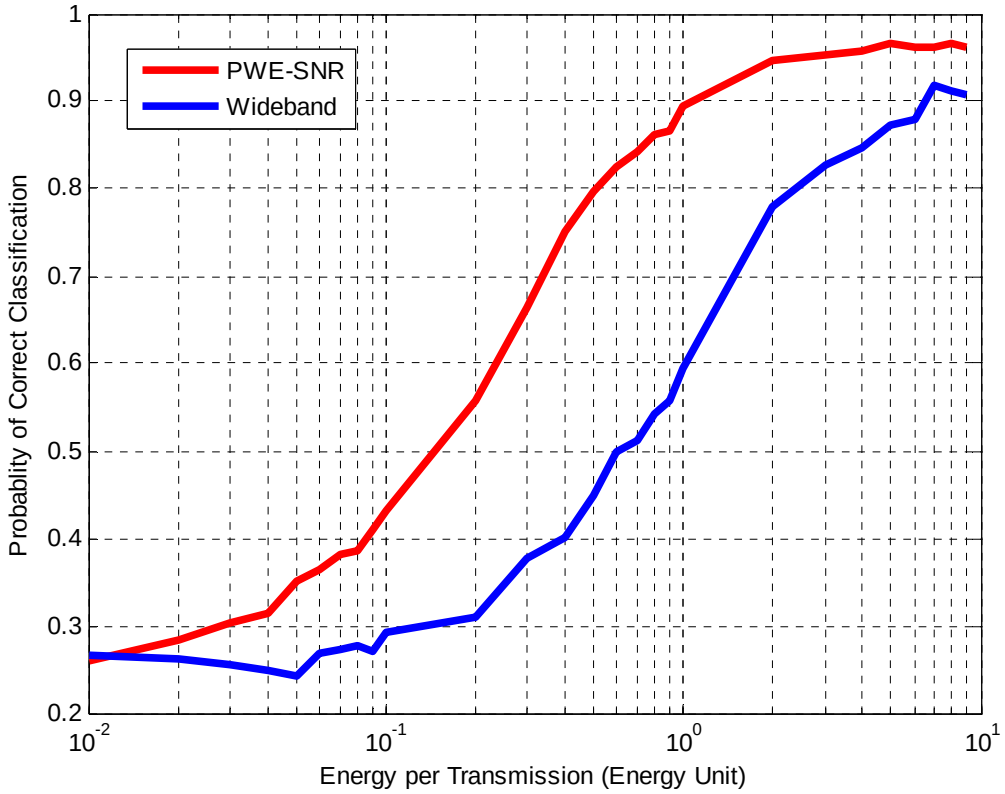

Figure 34. Classification performance curves of the optimized SNR illumination waveform and a traditional wideband waveform with the implementation of the NGCCR system for one transmission. Target distributions: Rayleigh, exponential, Gamma, log-normal. Monte Carlo setup: 50 target realizations; ten noise realizations. NGCCR setup: 40 online target realizations for the ensemble averaging.

The Monte Carlo experimental result for ten radar transmissions is presented in Figure 35. The Monte Carlo simulation is set to generate 50 target realizations and ten noise realizations for each target realization. The number of the online target realizations for the expected value estimation is set to $N_g = 40$. The P_{cc} for both illumination waveforms have improved in this case. For four target hypotheses that are Rayleigh, exponential, Gamma, and log-normal distributed, respectively, the PWE illumination waveform outperforms the traditional wideband illumination waveform by approximately

4 dB in transmission energy when P_{cc} is 90%. Another way to view the performance gain is that for a given mid-range transmission energy, we achieve approximately a 100% increase in P_{cc}. At very low energy levels, the receiver can no longer obtain any useful information from the received data since the AWGN in the receiver is the dominant component. At very high energy levels, the wideband illumination waveform has a 100% P_{cc}. However, the PWE illumination waveform only has a near 100% P_{cc}. One of the reasons may be that more Monte Carlo averaging is needed. For majority of the time, the PWE illumination waveform is still the better choice. Again, the P_{cc} curves for the non-Gaussian distributed targets are very similar to the P_{cc} curves for the Gaussian distributed targets. This result also shows the effectiveness of the NGCCR detection algorithm for classifying non-Gaussian targets.

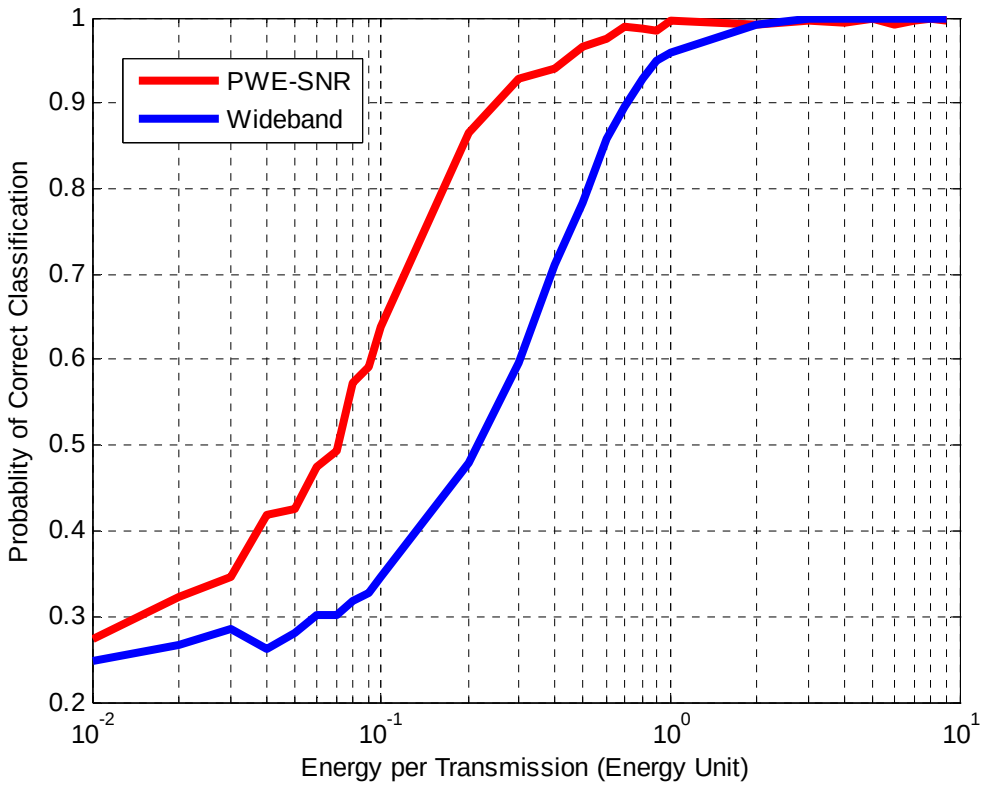

Figure 35. Classification performance curves of the optimized SNR illumination waveform and a traditional wideband waveform with the implementation of the NGCCR system for ten transmissions. Target distributions: Rayleigh, exponential, Gamma, log-normal. Monte Carlo setup: 50 target realizations; ten noise realizations. NGCCR setup: 40 online target realizations for the ensemble averaging.

Overall, we can draw conclusion from the results from these experimental test runs that the PWE illumination waveform outperforms the traditional wideband illumination waveform in an energy constraint environment due to the efficient use of the energy in the illumination waveforms. The new proposed NGCCR target classification scheme performs well with both Gaussian and non-Gaussian distributed complex stochastic targets compared to wideband illumination waveform. In the next chapter, we present conclusions and discuss topics for future research.

VII. CONCLUSIONS AND RECOMMENDATIONS

Romero et al. recently developed a new multiple hypothesis cognitive radar target classification algorithm (dubbed here the GCCR system) that exploits the spectral sparsity of correlated narrowband target responses to achieve significant performance improvements over traditional radars that use wideband illumination pulses.

The theory of the GCCR system to deal effectively with arbitrary zero-mean non-Gaussian distributed target responses was generalized in this thesis. The new algorithm is dubbed the NGCCR system. As discussed in Chapter 3, the GCCR system exploits Gaussian-motivated closed-form expressions to evaluate the joint density of the multiple measurements in integral form

$$\begin{aligned} p_i^k\left(\underline{y}_1, \underline{y}_2, \ \ldots, \underline{y}_k\right) &= E_{\underline{g}}\left\{p_i^k\left(\underline{y}_1, \underline{y}_2, \ldots, \underline{y}_k \left| \underline{g}_i \right.\right)\right\} \\ &= \int_{\underline{g}_i} p_i^k\left(\underline{y}_1, \underline{y}_2, \ldots, \underline{y}_k \left| \underline{g}_i \right.\right) p(\underline{g}_i) d\underline{g}_i . \end{aligned} \tag{56}$$

The NGCCR system relaxes the Gaussian target assumption. In this case, we cannot evaluate the expected value in integral form since there exists no closed-form expression for the integrand. The desired generalization was achieved via two key contributions. First, the joint density of the multiple measurements is evaluated numerically by replacing the integral with an ensemble averaging operation to evaluate the expected value of the joint condition posterior density of the measurements conditioned on the target realization given by

$$\begin{aligned} p_i^k\left(\underline{y}_1, \underline{y}_2, \ \ldots, \underline{y}_k\right) &= E_{\underline{g}}\left\{p_i^k\left(\underline{y}_1, \underline{y}_2, \ldots, \underline{y}_k \left| \underline{g}_i \right.\right)\right\} \\ &\approx \frac{1}{N_{\underline{g}}} \sum_{j=1}^{N_g} p_{i,j}^k\left(\underline{y}_1, \underline{y}_2, \ldots, \underline{y}_k \left| \underline{g}_i \right.\right). \end{aligned} \tag{57}$$

Next, a powerful new statistical sampling algorithm by Nichols et al. and a kernel density estimator were applied to draw complex target samples from target distributions specified by *both* desired power spectral densities and arbitrary desired probability density functions. These realizations are then used to form the ensemble of posterior density

values employed in the ensemble average operation. The NGCCR system requires prior knowledge of the target classes in the form of target response measurements or simulations based upon measurements. Given these measurements, it is possible to estimate the PDFs of the target classes using an appropriate PDF estimator (i.e., the kernel density estimator [19]. For this thesis, these PDF estimates were computed to aid visual analysis of the data and to gain insight; however, they were not used in the NGCCR system because they were not required for the implementation. In an operational scenario in which the target distributions are not known a priori, these PDFs can be estimated and used as part of the statistical sampling algorithm. Thus, the NGCCR system does not require prior knowledge of the "true" target distributions. If we are given representative measurements of the desired target responses (as we are in typical operational scenarios), we can estimate their PDFs, then draw target samples from their associated distributions, and use those target samples to evaluate the desired joint densities required above. Once we have these joint densities, we use them to update the prior probabilities. Next, we use the updated priors to update the PWE illumination signal, which is then transmitted by the radar to illuminate the targets. The user defines in advance the desired number of iterations to use. When that number of iterations is complete, the final target classification decision is made.

Simulations using non-Gaussian targets demonstrated very effective classification algorithm performance. As expected, this performance gain is realized at the expense of increased computational complexity.

Recommended future research lies in three main areas.

First, future research should focus on finding ways to reduce the computational complexity of the new algorithm.

Second, in addition, our current statistical sampling algorithm is limited to being able to sample from distributions that are specified by both a desired *symmetric* PSV and a desired PDF. Future work should also focus on creating a generalized method for sampling a distribution specified by both a desired *asymmetric* PSV and a desired PDF. This will likely involve using a phase retrieval algorithm for evaluating the IFT of a PSV.

Third, a demonstration of the full end-to-end process of generating target samples from a representative arbitrarily distributed target process should be conducted. This specific exercise was not conducted for the thesis. Assuming we are given only representative measurements from a target process, we need to estimate the PDF of the target distribution using a kernel density estimator. Next, we should draw IID samples from the target process using a statistical sampling algorithm such as the Importance Sampling algorithm or the Metropolis-Hastings Sampling algorithm. These IID samples should next be inserted into the Nichols sampling algorithm, along with the desired PSV. The results of the Nichols algorithm will be target samples that have both the desired arbitrary PDF and the desired PSV. Completion of this exercise will demonstrate that in an operational scenario, no prior knowledge of the target distribution is necessary. Clearly, the gains made by demonstrating this capability will be realized at the expense of greatly increased computational complexity.

THIS PAGE INTENTIONALLY LEFT BLANK

APPENDIX

This code was written to generate the four PSVs of the target hypotheses and evaluate the target generating function.

```
% Author Kenan Wang

% generate non-Gaussian colored spectra complex signals for the CR
% experiment

    close all;
    clear;
    clc;

%~~~~~~~~~~~~~~~~~~~~~~~~~~~~~~~~~~~~~~~~~~~~~~~~~~~~~~~~~~~~~~~~~~~~~~~~~~~~~~~
    N = 64; % define the number of samples in the signal sequence

    Ps = 1; % define the power of the signal
%~~~~~~~~~~~~~~~~~~~~~~~~~~~~~~~~~~~~~~~~~~~~~~~~~~~~~~~~~~~~~~~~~~~~~~~~~~~~~~~
% define the frequency bands for the bandpass PSD, the frequency is
% normalized to 0.5 Hz
%~~~~~~~~~~~~~~~~~~~~~~~~~~~~~~~~~~~~~~~~~~~~~~~~~~~~~~~~~~~~~~~~~~~~~~~~~~~~~~~
    mu1 = 0.2;
    mu2 = 0.3;
    mu3 = 0.35;
    mu4 = 0.4;
%~~~~~~~~~~~~~~~~~~~~~~~~~~~~~~~~~~~~~~~~~~~~~~~~~~~~~~~~~~~~~~~~~~~~~~~~~~~~~~~
% define the bandwidth of the PSD, different sigma will result in different
% amplitude and bandwidth of the PSD
%~~~~~~~~~~~~~~~~~~~~~~~~~~~~~~~~~~~~~~~~~~~~~~~~~~~~~~~~~~~~~~~~~~~~~~~~~~~~~~~
    sigma1 = 0.03;
    sigma2 = 0.02;
    sigma3 = 0.025;
    sigma4 = 0.015;
%~~~~~~~~~~~~~~~~~~~~~~~~~~~~~~~~~~~~~~~~~~~~~~~~~~~~~~~~~~~~~~~~~~~~~~~~~~~~~~~
% define the four pdfs we want the complex targets to draw samples from
% so far only these four options are allow. Adding options requires the
% changing of code in the function “generate_targets.m”
% pdf options are: ‘rayleigh’,’exponential’,’gamma’,and ‘lognorm’
%~~~~~~~~~~~~~~~~~~~~~~~~~~~~~~~~~~~~~~~~~~~~~~~~~~~~~~~~~~~~~~~~~~~~~~~~~~~~~~~

    pdf1 = ‘rayleigh’;
    pdf2 = ‘exponential’;
    pdf3 = ‘gamma’;
    pdf4 = ‘lognorm’;
%~~~~~~~~~~~~~~~~~~~~~~~~~~~~~~~~~~~~~~~~~~~~~~~~~~~~~~~~~~~~~~~~~~~~~~~~~~~~~~~
% define the normalized frequency domain
%~~~~~~~~~~~~~~~~~~~~~~~~~~~~~~~~~~~~~~~~~~~~~~~~~~~~~~~~~~~~~~~~~~~~~~~~~~~~~~~
    df = 1/N;
    f = -0.5:df:0.5-df;
%~~~~~~~~~~~~~~~~~~~~~~~~~~~~~~~~~~~~~~~~~~~~~~~~~~~~~~~~~~~~~~~~~~~~~~~~~~~~~~~
% compute the four proposed PSDs
%~~~~~~~~~~~~~~~~~~~~~~~~~~~~~~~~~~~~~~~~~~~~~~~~~~~~~~~~~~~~~~~~~~~~~~~~~~~~~~~
    Sxx1 = (Ps/(2*sqrt(2*pi)*sigma1))*(exp(-(f-mu1).^2/(2*sigma1^2))+exp(-
(f+mu1).^2/(2*sigma1^2)));
    Sxx2 = (Ps/(2*sqrt(2*pi)*sigma2))*(exp(-(f-mu2).^2/(2*sigma2^2))+exp(-
(f+mu2).^2/(2*sigma2^2)));
```

```
    Sxx3 = (Ps/(2*sqrt(2*pi)*sigma3))*(exp(-(f-mu3).^2/(2*sigma3^2))+exp(-
(f+mu3).^2/(2*sigma3^2)));
    Sxx4 = (Ps/(2*sqrt(2*pi)*sigma4))*(exp(-(f-mu4).^2/(2*sigma4^2))+exp(-
(f+mu4).^2/(2*sigma4^2)));
%~~~~~~~~~~~~~~~~~~~~~~~~~~~~~~~~~~~~~~~~~~~~~~~~~~~~~~~~~~~~~~~~~~~~~~~~~~~~~~~~
% plot the four proposed PSDs
%~~~~~~~~~~~~~~~~~~~~~~~~~~~~~~~~~~~~~~~~~~~~~~~~~~~~~~~~~~~~~~~~~~~~~~~~~~~~~~~~
    figure
    subplot(221)
    plot(f,Sxx1);
    ylabel('Sxx1(f)')
    xlabel('Normalized Frequency')
    title('Target Hypothesis #1')
    subplot(222)
    plot(f,Sxx2);
    ylabel('Sxx2(f)')
    xlabel('Normalized Frequency')
    title('Target Hypothesis #2')
    subplot(223)
    plot(f,Sxx3);
    ylabel('Sxx3(f)')
    xlabel('Normalized Frequency')
    title('Target Hypothesis #3')
    subplot(224)
    plot(f,Sxx4);
    ylabel('Sxx4(f)')
    xlabel('Normalized Frequency')
    title('Target Hypothesis #4')
%~~~~~~~~~~~~~~~~~~~~~~~~~~~~~~~~~~~~~~~~~~~~~~~~~~~~~~~~~~~~~~~~~~~~~~~~~~~~~~~~
% simulate four target realizations based on the proposed pdf and PSDs
%~~~~~~~~~~~~~~~~~~~~~~~~~~~~~~~~~~~~~~~~~~~~~~~~~~~~~~~~~~~~~~~~~~~~~~~~~~~~~~~~
    h1 = generate_targets( Sxx1, pdf1, N) + 1j*generate_targets( Sxx1, pdf1, N);
    %h1 = h1 - mean(h1);
    h2 = generate_targets( Sxx2, pdf2, N) + 1j*generate_targets( Sxx2, pdf2, N);
    %h2 = h2 - mean(h2);
    h3 = generate_targets( Sxx3, pdf3, N) + 1j*generate_targets( Sxx3, pdf3, N);
    %h3 = h3 - mean(h3);
    h4 = generate_targets( Sxx4, pdf4, N) + 1j*generate_targets( Sxx4, pdf4, N);
    %h4 = h4 - mean(h4);
%~~~~~~~~~~~~~~~~~~~~~~~~~~~~~~~~~~~~~~~~~~~~~~~~~~~~~~~~~~~~~~~~~~~~~~~~~~~~~~~~
% compute the PSV of the four realized target and plot the results
%~~~~~~~~~~~~~~~~~~~~~~~~~~~~~~~~~~~~~~~~~~~~~~~~~~~~~~~~~~~~~~~~~~~~~~~~~~~~~~~~
    H1 = abs(fftshift(fft(h1))).^2;
    H2 = abs(fftshift(fft(h2))).^2;
    H3 = abs(fftshift(fft(h3))).^2;
    H4 = abs(fftshift(fft(h4))).^2;

    figure
    subplot(221)
    plot(f,H1)
    ylabel('Sxx1(f)')
    xlabel('Normalized Frequency')
    title('Target #1')
    subplot(222)
    plot(f,H2)
    ylabel('Sxx2(f)')
    xlabel('Normalized Frequency')
    title('Target #2')
    subplot(223)
    plot(f,H3)
    ylabel('Sxx3(f)')
    xlabel('Normalized Frequency')
```

```
    title('Target #3')
    subplot(224)
    plot(f,H4)
    ylabel('Sxx4(f)')
    xlabel('Normalized Frequency')
    title('Target #4')

%~~~~~~~~~~~~~~~~~~~~~~~~~~~~~~~~~~~~~~~~~~~~~~~~~~~~~~~~~~~~~~~~~~~~~~~~~~~~~~~
% the following code allow you to see the pdf estimates, the time waveform
% and the normplots of the four complex target signals
%~~~~~~~~~~~~~~~~~~~~~~~~~~~~~~~~~~~~~~~~~~~~~~~~~~~~~~~~~~~~~~~~~~~~~~~~~~~~~~~

    [f_h1_real hi1_real] = ksdensity(real(h1));
    [f_h1_imag hi1_imag] = ksdensity(imag(h1));
    [f_h2_real hi2_real] = ksdensity(real(h2));
    [f_h2_imag hi2_imag] = ksdensity(imag(h2));
    [f_h3_real hi3_real] = ksdensity(real(h3));
    [f_h3_imag hi3_imag] = ksdensity(imag(h3));
    [f_h4_real hi4_real] = ksdensity(real(h4));
    [f_h4_imag hi4_imag] = ksdensity(imag(h4));

    figure
    subplot(421)
    plot(hi1_real, f_h1_real)
    ylabel('p(real(h1))')
    xlabel('real(h1)')
    subplot(422)
    plot(hi1_imag, f_h1_imag)
    ylabel('p(imag(h1))')
    xlabel('imag(h1)')
    subplot(423)
    plot(hi2_real, f_h2_real)
    ylabel('p(real(h2))')
    xlabel('real(h2)')
    subplot(424)
    plot(hi2_imag, f_h2_imag)
    ylabel('p(imag(h2))')
    xlabel('imag(h2)')
    subplot(425)
    plot(hi3_real, f_h3_real)
    ylabel('p(real(h3))')
    xlabel('real(h3)')
    subplot(426)
    plot(hi3_imag, f_h3_imag)
    ylabel('p(imag(h3))')
    xlabel('imag(h3)')
    subplot(427)
    plot(hi4_real, f_h4_real)
    ylabel('p(real(h4))')
    xlabel('real(h4)')
    subplot(428)
    plot(hi4_imag, f_h4_imag)
    ylabel('p(imag(h4))')
    xlabel('imag(h4)')

    figure
    subplot(421)
    plot(real(h1))
    title('time waveform of real(h1)')
    ylabel('real(h1)')
    xlabel('n')
    subplot(422)
```

```
    plot(imag(h1))
    title('time waveform of imag(h1)')
    ylabel('imag(h1)')
    xlabel('n')
    subplot(423)
    plot(real(h2))
    title('time waveform of real(h2)')
    ylabel('real(h2)')
    xlabel('n')
    subplot(424)
    plot(imag(h2))
    title('time waveform of imag(h2)')
    ylabel('imag(h2)')
    xlabel('n')
    subplot(425)
    plot(real(h3))
    title('time waveform of real(h3)')
    ylabel('real(h3)')
    xlabel('n')
    subplot(426)
    plot(imag(h3))
    title('time waveform of imag(h3)')
    ylabel('imag(h3)')
    xlabel('n')
    subplot(427)
    plot(real(h4))
    title('time waveform of real(h4)')
    ylabel('real(h4)')
    xlabel('n')
    subplot(428)
    plot(imag(h4))
    title('time waveform of imag(h4)')
    ylabel('imag(h4)')
    xlabel('n')

    figure
    subplot(221)
    normplot(real(h1))
    subplot(222)
    normplot(imag(h1))
    subplot(223)
    normplot(real(h2))
    subplot(224)
    normplot(imag(h2))

    figure
    subplot(221)
    normplot(real(h3))
    subplot(222)
    normplot(imag(h3))
    subplot(223)
    normplot(real(h4))
    subplot(224)
    normplot(imag(h4))

%~~~~~~~~~~~~~~~~~~~~~~~~~~~~~~~~~~~~~~~~~~~~~~~~~~~~~~~~~~~~~~~~~~~~~~~~~~~~~~~~
% save the PSV and the names of the pdfs of the targets for the experiment
%~~~~~~~~~~~~~~~~~~~~~~~~~~~~~~~~~~~~~~~~~~~~~~~~~~~~~~~~~~~~~~~~~~~~~~~~~~~~~~~~
    Sxx = [Sxx1' Sxx2' Sxx3' Sxx4'];
    pdf_names = {pdf1 pdf2 pdf3 pdf4};
    save('targets.mat','Sxx','pdf_names')
```

This code was written for the Monte Carlo simulation of the multiple hypothesis target classification algorithm. The PWE and the wideband illumination waveforms are used for comparisons.

```
% Author: Kenan Wang

% Case: non-Gaussian stochastic targets in AWGN
% Waveform Design: Uses PWE (probability weighted energy)

% Target Recognition Experiment
% Estimate of the maximum likelihood Detection

close all;
clear;
clc;

%%%%%%%%%%%%%%%%%%%%%%%%%%%%%%%%%%%%%%%%%%%%%%%%%%%%%%%%%%%%%%%%%%%%%%%%%%%%%%%%
% INITIALIZATIONS:  The user should choose parameters here
%%%%%%%%%%%%%%%%%%%%%%%%%%%%%%%%%%%%%%%%%%%%%%%%%%%%%%%%%%%%%%%%%%%%%%%%%%%%%%%%



%~~~~~~~~~~~~~~~~~~~~~~~~~~~~~~~~~~~~~~~~~~~~~~~~~~~~~~~~~~~~~~~~~~~~~~~~~~~~~~~~
% Monte Carlo loop parameters
%~~~~~~~~~~~~~~~~~~~~~~~~~~~~~~~~~~~~~~~~~~~~~~~~~~~~~~~~~~~~~~~~~~~~~~~~~~~~~~~~
    target_realization = 50;    % Number of target realizations
    num_exp            = 10;    % Number of noise realizations
    Ntheta             = 4;     % No.of target hypotheses (this is fixed)
%~~~~~~~~~~~~~~~~~~~~~~~~~~~~~~~~~~~~~~~~~~~~~~~~~~~~~~~~~~~~~~~~~~~~~~~~~~~~~~~~

transmission       = 10;     % Number of radar transmissions
num_ensemble       = 40;    % Number of the target realizations used in the
                            % online ensemble to calculate the expected
                            % value of the difference between the received
                            % data and the target hypotheses
                            % this number is good for 10-40 but above 25
                            % will see very consistent results



load targets;               % load the PSV of the target hypotheses
                            % this .mat file contains the Sxx and the name
                            % of the target distributions


Lsignal = length(Sxx);      % obtain the length of the signal
Ly      = Lsignal*2-1;      % compute the length of the convolution between
                            % the input and the signal process

Pn = 1;                  % Noise power, setting it to 1 will give TNR = 10dB
var_noise = sqrt(Pn/2);     % compute the variance of the noise
Kn     = var_noise*eye(Ly); % compute the covariance matrix of the noise

N       = Lsignal;          % rename the variable for convenience
```

```
ES = energy_levels(1e-2,10); % define the range of the levels of energy for the
radar transmitter
                             % that we want to run the experiment on
                             % the first argument is the lower bound and the
                             % second argument is the upperbound

accuracy = zeros(1,length(ES));         % Memory allocation for the accuracy
vector
final_result = zeros(2,length(ES));     % Memory allocation for the final
result vector

dec                          = 0;       % initialize the decision variable
loop_track                   = 0;       % a variable to track the num. of loops
for the experiment

%~~~~~~~~~~~~~~~~~~~~~~~~~~~~~~~~~~~~~~~~~~~~~~~~~~~~~~~~~~~~~~~~~~~~~~~~~~~~~~~
% SNR CASE WITH NO CLUTTER:
% Compute the Optimal Input Signal xi(t) for each of the Target
% Hyptheses i = 1, 2, ..., M, where M = Nthetha in the code
% the second argument indicates whether the the target hypotheses are in the
frequency
% domain or the time domain. 0 for frequency domain, 1 for time domain
%~~~~~~~~~~~~~~~~~~~~~~~~~~~~~~~~~~~~~~~~~~~~~~~~~~~~~~~~~~~~~~~~~~~~~~~~~~~~~~~

    x_opt = opt_waveforms(Sxx',0);


%~~~~~~~~~~~~~~~~~~~~~~~~~~~~~~~~~~~~~~~~~~~~~~~~~~~~~~~~~~~~~~~~~~~~~~~~~~~~~~~
% Create a complex wideband input
%~~~~~~~~~~~~~~~~~~~~~~~~~~~~~~~~~~~~~~~~~~~~~~~~~~~~~~~~~~~~~~~~~~~~~~~~~~~~~~~
    delta = zeros(Lsignal,1);
    delta(1) = 1;
    delta = delta + 1j*delta;
    delta = delta/sqrt(delta'*delta);



for k1 = 1:2 % perform this process twice. first time is the PWE input method,
the second time is the wideband method

    if (k1 == 1)
        waveform_method = 'PWE';    % Define the waveform method used
    else
        waveform_method = 'wideband';
    end


    for k2 = 1:length(ES)              % perform target classification at each
energy level


        Es = ES(k2) ;                  % Energy per transmission

        for k3 = 1:Ntheta              % Monte Carlo loop for the four target
hypotheses

            err = 0;                   % initialize the error

            hypo = k3;                 % set the hypo equal to the defined
hypothesis
```

```
            for k4 = 1:target_realization % Monte Carlo loop for number of
target realizations

                %~~~~~~~~~~~~~~~~~~~~~~~~~~~~~~~~~~~~~~~~~~~~~~~~~~~~~~~~~~~
                % an algorithm to generate the non-Gaussian targets based
                % on the current hypothesis
                %~~~~~~~~~~~~~~~~~~~~~~~~~~~~~~~~~~~~~~~~~~~~~~~~~~~~~~~~~~~
                    switch hypo
                        case 1
                            h = generate_targets( Sxx(:,1)', char(pdf_names(1)),
N) + 1j*generate_targets( Sxx(:,1)', char(pdf_names(1)), N);
                        case 2
                            h = generate_targets( Sxx(:,2)', char(pdf_names(2)),
N) + 1j*generate_targets( Sxx(:,2)', char(pdf_names(2)), N);
                        case 3
                            h = generate_targets( Sxx(:,3)', char(pdf_names(3)),
N) + 1j*generate_targets( Sxx(:,3)', char(pdf_names(3)), N);
                        case 4
                            h = generate_targets( Sxx(:,4)', char(pdf_names(4)),
N) + 1j*generate_targets( Sxx(:,4)', char(pdf_names(4)), N);
                    end

                    h = h';         % remove the mean

                %~~~~~~~~~~~~~~~~~~~~~~~~~~~~~~~~~~~~~~~~~~~~~~~~~~~~~~~~~~~

                for k5 = 1:num_exp % Monte Carlo loop for number of noise
realizations

                    loop_track = loop_track + 1;        % increment on the
number of loops
                    ptheta      = zeros(Ntheta,1);      % Vector: Allocate
memory for the prior probabilities
                    ptheta(:,1) = 1/Ntheta;             % RR: initial priors
                                                        % Since we have no
prior knowledge, we assume that the
                                                        % priors are all equal
                    cond_y_h = mp(ones(Ntheta,1));      % initialize the
variable p(y|h)

                    for k6 = 1:transmission % Number of radar transmissions

                        noise       = sqrt(Pn/2)*(randn(Ly,1)+
1j*randn(Ly,1)); % generate complex noise Pn is noise power

 % the variance of the noise is Pn/2

                        switch waveform_method % Generate the optimal waveforms
and simulate the data measurement
                            case 'PWE',
                                x_input         =
sqrt(Es)*x_opt*sqrt(ptheta(:,k6)); % PWE with proper scaling
                                y               = conv(x_input,h) +
noise;           % simulate the data measurement
                            case 'wideband'
                                x_input         =
sqrt(Es)*delta;                  % wideband with proper scaling
                                y               = conv(x_input,h) +
noise;           % simulate the data measurement
                        end

                    %~~~~~~~~~~~~~~~~~~~~~~~~~~~~~~~~~~~~~~~~~~~~~~~~~~~~~~~~
```

```
                    % Compute the “pdf”
                    %~~~~~~~~~~~~~~~~~~~~~~~~~~~~~~~~~~~~~~~~~~~~~~~~~~~~~~~~

                        for k7 = 1:Ntheta

                            %~~~~~~~~~~~~~~~~~~~~~~~~~~~~~~~~~~~~~~~~~~~~~~~~
                            % use online ensemble averaging to compute
                            % Eg[p(y1,...,yk)]
                            % the mp function is part of the multiprecision
                            % computing toolbox
                            %~~~~~~~~~~~~~~~~~~~~~~~~~~~~~~~~~~~~~~~~~~~~~~~~
                                for k8 = 1:num_ensemble

                                    % Generate a target based on one of the
                                    % hypothesis
                                    hi              =
generate_targets( Sxx(:,k7)’, char(pdf_names(k7)), N) +
1j*generate_targets( Sxx(:,k7)’, char(pdf_names(k7)), N);
                                    hi              = h’;

                                    % compute exp[(y-Xg)’Kn^-1(y-Xg)]
                                    yi              = conv(x_input,hi);
                                    w               = -(y - yi)’/Kn*(y - yi);
                                    z(k8)           = cond_y_h(k7)*exp(w);
                                end

                                % compute the expected values of the
                                % ensemble average
                                    cond_y_h(k7)       = mean(z);

                        end % end loop for computing pdf for one hypothesis

                        % the result is the pdf for the estimate of the
                        % maximum likelihood detection algorithm
                            pdf      = cond_y_h;

                        %~~~~~~~~~~~~~~~~~~~~~~~~~~~~~~~~~~~~~~~~~~~~~~~~~~~~~~~~
                        % UPDATE THE PRIORS
                        %~~~~~~~~~~~~~~~~~~~~~~~~~~~~~~~~~~~~~~~~~~~~~~~~~~~~~~~~

                            % RR: update ptheta and normalize it
                            ptheta(:,k6+1) =
real(vpa(ptheta(:,1).*pdf/sum(ptheta(:,1).*pdf),2));  % Vector (i x k)
                            ptheta(:,k6+1) = round(ptheta(:,k6+1)*100)/100;  %
round the percentage to 2 decimal points

                        %~~~~~~~~~~~~~~~~~~~~~~~~~~~~~~~~~~~~~~~~~~~~~~~~~~~~~~~~

                    end % end loop for one radar transmission

                    %%%%%%%%%%%%%%%%%%%%%%%%%%%%%%%%%%%%%%%%%%%%%%%%%%%%%%%%
                    % the target will have the maximum ptheta value
                    %%%%%%%%%%%%%%%%%%%%%%%%%%%%%%%%%%%%%%%%%%%%%%%%%%%%%%%%

                        [pr,dec] = max(ptheta(:,transmission+1)); % dec = index
corresponding to the max prior probability

                    %%%%%%%%%%%%%%%%%%%%%%%%%%%%%%%%%%%%%%%%%%%%%%%%%%%%%%%%
                    % Error calcuation
                    %%%%%%%%%%%%%%%%%%%%%%%%%%%%%%%%%%%%%%%%%%%%%%%%%%%%%%%%

                        if(dec ~= hypo)
```

```
                        err = err + 1;
                    end

                    %%%%%%%%%%%%%%%%%%%%%%%%%%%%%%%%%%%%%%%%%%%%%%%%%%%%%%%%

                    loop_remain =
round((num_exp*target_realization*Ntheta*length(ES)*2-loop_track)); % loop
track
                    clc;
                    sprintf('loop remain: %d loops.', loop_remain) % display
the num. of loops remain

                end % end loop for one noise realization

            end % end loop for one target realization

            error_rate(k3) = err/(target_realization*num_exp); % compute the
error rate for one hypothesis

        end % end loop for one target hypothesis

        error_rate_total = sum(error_rate)/Ntheta;              % average the
error rate for the four hypotheses

        accuracy(k2) = 1 - error_rate_total;                    % compute P(CC)
= 1-P(error)

    end % end loop for one energy level (Es)

    final_result(k1,:) = accuracy;                              % assign P(CC)
for the result of one energy level

end % end loop for the two options of the waveform methods

    %~~~~~~~~~~~~~~~~~~~~~~~~~~~~~~~~~~~~~~~~~~~~~~~~~~~~~~~~~~~~~~~~~~~~~~~~
    % plot the final_result
    %~~~~~~~~~~~~~~~~~~~~~~~~~~~~~~~~~~~~~~~~~~~~~~~~~~~~~~~~~~~~~~~~~~~~~~~~

        semilogx(ES,final_result,'LineWidth',2);
        ylim([0.2 1])
        xlabel('Energy per Transmission')
        ylabel('Probablity of Correct Classification')
        final_title1 = 'Classification Performance with %d Transmissions';
        final_title2 = '\n%d Target Realization/ %d Noise Realization';
        final_title3 = '\n%d Online Target Ensemble Averaging';
        final_title = [final_title1 final_title2 final_title3];

title(sprintf(final_title,transmission,target_realization,num_exp,num_ensemble))
        legend('PWE','Wideband');

    %%%%%%%%%%%%%%%%%%%%%%%%%%%%%%%%%%%%%%%%%%%%%%%%%%%%%%%%%%%%%%%%%%%%%%%%
    % END OF CODE
    %%%%%%%%%%%%%%%%%%%%%%%%%%%%%%%%%%%%%%%%%%%%%%%%%%%%%%%%%%%%%%%%%%%%%%%%
```

This code is written for generating a vector of energy levels specified by the minimum and maximum bounds.

```
function [ Es ] = energy_levels( Es_min, Es_max )

% create 10 energy levels for 1 decibel
ES = zeros(1,9);
for i = 1:9
    ES(i) = Es_min*i;
end

Es_range = Es_max/Es_min;
num_decibel = log10(Es_range);

ES_initial   = ES;
%ES_current   = zeros(1,9*num_decibel);
ES_current   = ES_initial;

for i = 1:(num_decibel-1)
    ES_next = ES_initial*10^i;
    ES_current = [ES_current ES_next];
end

Es = ES_current;

end
```

This is the code written to generate real signals with both specified PDFs and specified PSVs. This code was written by Nichols et al. [8].

```
function [ x ] = generate_targets( Sxx, pdf, N)

Sxx(N/2+1)=0; % zero out the DC component (remove mean)
Xf = sqrt(Sxx);   % Convert PSD to Fourier amplitudes
Xf=ifftshift(Xf); % Put in Matlab FT format

switch pdf
    case 'gaussian'
        x = randn(1,N);
    case 'rayleigh'
        x = raylrnd(10,[1,N]); % generate N iid samples conforming to p(x)
    case 'exponential'
        x = exprnd(2,[1,N]);
    case 'gamma'
        x = gamrnd(2,2,[1,N]);
    case 'lognorm'
        x = lognrnd(0, 1, [1,N]);
end

vs = sum(Sxx/N)*(N/(N-1)); % define the signal variance based on the PSD

x=x*sqrt(vs/var(x)); % guarantee new data match this variance
```

```
mx=mean(x);

x=x-mx; % subtract the mean

[xo,~]=sort(x); % store sorted signal xo with correct p(x)

k=1;
indxp=zeros(1,N); % initialize counter

while(k)
    Rk=fft(x); % Compute FT
    Rp=atan2(imag(Rk),real(Rk)); % Get phases
    x=real(ifft((exp(1j.*Rp)).*abs(Xf))); % Give signal correct PSD
    [~,indx]=sort(x); % Get rank of signal with correct PSD
    x(indx)=xo; % rank reorder (simulate nonlinear transform)
    k=k+1; % increment counter
    if(indx==indxp)
        k=0;
    end % if we converged, stop
    indxp=indx; % re-set ordering for next iter
end
%x=x+mx; % Put back in the mean
x = x/sqrt(2*N);

end
```

This is the code written to generate optimal illumination waveform based on the proposed target hypotheses. This code was written by R. Romero [4].

```
function [ x_opt ] = opt_waveforms( target_hypotheses , time_domain)


    hh = target_hypotheses;                 % reassign the variables
    N       = length(hh);



    if time_domain

        [~,Ntheta] = size(target_hypotheses);   % obtain the number of
hypotheses

        H = fft(hh);                            % calculate the fft of the
target response
                                                % (GAC_KNW): Matrix: This
computes the four
                                                % target transfer functions
corresponding to the four target signals

        Sf = abs(H).^2;                         % (RR):calculate the impulse
response
                                                % (GAC_KNW): Matrix - We
Compute the Magnitude squared of the
                                                % transfer functions of the
targets

    else
```

```
        [Ntheta, ~] = size(target_hypotheses); % obtain the number of
hypotheses
        Sf = zeros(length(hh),Ntheta);
        for i = 1:Ntheta
            H = hh(i,:);
            Sf(:,i) = ifftshift(H);
        end
    end

    L = length(Sf);                         % Length of impulse response
                                            % Length of the Mag. Sqrd of the
Target
                                            % Transfer Functions

    df = 1/L;                               % delta frequency (frequency sample
period)


                                            % Create a frequency vector and a
time vector
                                            % variables needed to form
autocorrelation
                                            % frequency(f) and time(n)

    f = (0:(L-1))*df;                       % normalized frequency from 0 to 1-
df
                                            % same as normalizing sampling time
1s
    n = (0:L-1)';                           % discrete time scale;

    V = exp(1j*2*pi*n*f);                   % frequency time vector
                                            % GAC: This is a matrix (31 x 31)
                                            % This is a Fourier Transform
kernel trick used in the Kay algorithm for
                                            % converting a PSD to a covariance
matrix under the Gaussian assumption
                                            % These are the eigenvectors used
by Kay


    Rh = zeros(L,L,Ntheta);                 % allocate memory for the
autocorrelation matrix
    x_opt = zeros(L,Ntheta);

    for i1 = 1:Ntheta,

        H2f = Sf(:,i1);         % Select one column out of the matrix
                                % Mag. Sqrd of Tranfer function |H(f)|^2 for
one target hypothesis

        Rh(:,:,i1) = (V*diag(df*H2f')*V');  % form the autocorrelation matrix

        [eig_max,~] = eigs(Rh(:,:,i1),1,'LM');    % find the maximum
eigenvector, which is the finite duration, energy constrained x(t) that
                                                  % maximizes SNR
        x_opt(:,i1) = eig_max/sqrt(eig_max'*eig_max);   % normalize the energy
in x_opt
    end
end
```

LIST OF REFERENCES

[1] S. Haykin, "Cognitive radar" in *IEEE Signal Processing Magazine*, vol. 30, January 2006.

[2] R. Romero and N. A. Goodman, "Information-theoretic matched waveform in signal dependent interference," in *Proc. of IEEE Radar Conference*, Rome, Italy, May 2008.

[3] R. Romero and N. A. Goodman, "Waveform design in signal-dependent interference and application to target recognition with multiple transmissions," *IET Radar Sonar Navig.*, vol. 3, no. 4, pp. 328–340, 2009.

[4] R. Romero and N. A. Goodman, "Improved waveform design for target recognition with multiple transmissions," presented at International WDD Conference, Orlando, Florida, 2009.

[5] R. Romero and N. A. Goodman, "Theory and application of SNR and mutual information matched illumination waveforms," *IEEE Trans. Aerosp. Electron. Syst.*, vol. 47, no. 2, 2011.

[6] M. R. Bell, "Information theory and radar waveform design," *IEEE Trans. on Information Theory*, vol. 39, no. 5, 1993.

[7] S. M. Kay, "Asymptotic Gaussian PDF" in *Fundamentals of Statistical Signal Processing*, Vol. 2, *Detection Theory*, Upper Saddle River: Prentice Hall PTR, pp. 33–38, 1998.

[8] J. M. Nichols, C. C. Olson, J. V. Michalowicz, and F. Bucholtz, "A simple algorithm for generating spectrally colored, non-Gaussian signals" in *Probabilistic Engineering Mechanics*, vol. 25, Elsevier, pp. 315–322, 2010.

[9] C. P. Robert and G. Casella, "Bayesian methods" in *Monte Carlo Statistical Methods*, 2nd ed. New York: Springer, ch. 1, sec. 3, pp. 12–18, 2004.

[10] J. V. Candy, *Bayesian signal processing classical, modern, and particle filtering methods*. New Jersey: Wiley, 2009.

[11] A. Papoulis and S. U. Pillai, *Probability, random variables and Stochastic processes* 4th ed., New York: McGraw-Hill, 2002.

[12] A. D. Whalen, *Detection of signals in noise*. New York: Academic Press, 1971.

[13] H. L. Van Trees, *Detection, estimation, and modulation theory*, Part 1. New York: John Wiley & Sons, 1968.

[14] G. L. Wise, A. P. Traganitis, and J. B. Thomas, “The effect of a memoryless nonlinearity on the spectrum of a random process,” *IEEE Trans. Inf. Theory*, IT-23, pp. 84–89, 1977.

[15] B. Liu, D. C. Munson Jr, “Generation of a random sequence having a jointly specified marginal distribution and autocovariance,” *IEEE Trans. Acoust., Speech, Signal Process.*, ASSP-30(6), pp. 973–983, 1982.

[16] U. G. Gujar and R. J. Kavanagh, “Generation of random signals with specified probability density functions and power density spectra,” *IEEE Trans Autom. Control*, AC-13, pp. 716–719, 1968.

[17] M. Shinozuka and C. M. Jan, “Digital simulation of random processes and its application,” *Journal of Sound and Vibration*, ch. 25, sec. 1, pp. 111–128, 1972.

[18] G. A. Clark, *Phase retrieval from modulus using homeomorphic signal processing and the complex cepstrum: an algorithm for lightning protection system*, Lawrence Livermore National Laboratory, Report UCRL-TR-205254, June 2004.

[19] B. W. Silverman, *Density estimation for statistics and data analysis*. New York: Chapman and Hall, 1986.

INITIAL DISTRIBUTION LIST

1. Defense Technical Information Center
   Ft. Belvoir, Virginia

2. Dudley Knox Library
   Naval Postgraduate School
   Monterey, California

3. R. Clark Robertson
   Naval Postgraduate School
   Monterey, California

4. Grace A. Clark
   Naval Postgraduate School
   Monterey, California

5. Ric A. Romero
   Naval Postgraduate School
   Monterey, California

6. Ke Nan Wang
   Naval Postgraduate School
   Monterey, California